

FINAL REPORT

Title: Improving post-wildfire peak streamflow predictions for small watersheds and communities

JFSP PROJECT ID: 19-1-01-55

June 2021

PI Alicia M. Kinoshita
San Diego State University
Civil, Construction, and Environmental Engineering

SI Brenton A. Wilder
San Diego State University
Civil, Construction, and Environmental Engineering



FIRESCIENCE.GOV
Research Supporting Sound Decisions



List of Abbreviations/Acronyms, Keywords

CAL FIRE	California Department of Forestry and Fire Protection
CGS	Department of Conservation – California Geological Survey
Chaparral Ecosystem	Characterized by the fire prone woody species that inhabit the wildlands of southern California
ECOSTRESS	ECOsystem Spaceborne Thermal Radiometer Experiment on Space Station
ET	Evapotranspiration
EVI	Enhanced Vegetation Index
HydroShare	Online repository for hydrologic data and models shared to the community
Machine Learning	Statistical based method that automates analytical model building
PT-JPL	Priestley-Taylor Jet Propulsion Laboratory Algorithm
Random Forest	Machine learning method that is used in classification and regression problems
RCS	Rowe, Countryman, and Storey (1949) method to predict post-fire peak flow
Small Watershed	Contributing area that drains to a point. A small watershed is defined as a drainage area less than 50 km ²
Soil Burn Severity	The effect of a fire on vegetation and soil conditions
SPI	Standardized Precipitation Index
SSEBop	Operational Simplified Surface Energy Balance model
USGS	United States Geological Survey
USFS	United States Forest Service
WY	Water Year, October 1 of previous year through September 30 of the given year

Abstract

Fire frequency and severity in southern California and across the western United States is increasing, posing a concern to the safety and well-being of communities and ecosystems. Increased aridity coupled with water stressed vegetation from prolonged droughts are leading to a higher propensity for larger, more intense fires that impact ecohydrological processes. Accurate characterization of these processes will improve rapid response efforts and long-term resource management to promote resilient communities along the wildland-urban interface. This work investigates prediction tools for small watersheds, where post-fire effects occur at a disproportional rate, by presenting methods to improve rapid predictions of post-fire streamflow and long-term monitoring of ecohydrological recovery. A random forest machine learning algorithm with 45 watershed parameters was created to predict post-fire peak streamflow for 1920 to 2019. This flood forecasting technique incorporated additional characteristics about meteorological and watershed properties to improve predictions of peak streamflow compared to flood frequency methods such as Rowe et al. (1949). The time elapsed after fire, peak hourly rainfall intensity, and drainage area were important factors that represented realistic conditions and increased accuracy of the random forest predictions. We used the case of the 2018 Holy Fire in southern California to characterize pre-fire climate and vegetation interactions and monitor post-fire recovery of ecohydrological processes (rainfall-runoff and evapotranspiration) for unburned (Santiago) and burned (Coldwater) catchments. ECOSystem Spaceborne Thermal Radiometer Experiment on Space Station (ECOSTRESS), Operational Simplified Surface Energy Balance Model (SSEBop), satellite-based vegetation indices, and local rainfall-runoff data were incorporated into our analyses. Consistent with the drought conditions in California from 2012 to 2018, we observed low precipitation and evapotranspiration prior to the fire. Further, large pre-fire vegetation biomass and areas containing montane hardwood species were more likely to be classified as high soil burn severity. Between ECOSTRESS and SSEBop there was larger variability in evapotranspiration estimates after fire compared to pre-fire, which had implications for post-fire vegetation recovery and water storage. The water balance highlighted variability in predicted storage between burned and unburned catchments, which was dependent on the evapotranspiration model used. ECOSTRESS PT-JPL model was more sensitive to parameters such as land surface temperature, net radiation, slope aspect, soil burn severity, and vegetation species due to higher spatial resolution. The findings of this research improves upon our current methods in modeling post-fire peak flows and post-fire vegetation recovery in southern California and has potential for future applications in management and planning.

Acknowledgements

This work is partially supported by the Joint Fire Science Program Graduate Research Innovation Award (#19-1-01-55) and Department of Conservation - California Geological Survey. We thank Dr. Kinoshita's Disturbance Hydrology Lab for insightful discussions, and students, Harmit Chima, Ubaldo Gonzalez, and Sydney Johnson from the Mathematics, Engineering, Science Achievement (MESA) 2019 Research Academy at San Diego State University for their contributions. We thank Christine Lee (National Aeronautics and Space Administration Jet Propulsion Laboratory (NASA JPL), Terrestrial Hydrology) and Paa Sey (NASA JPL Internship Student) for the insightful discussions regarding the use of ECOSTRESS in wildfire applications. We appreciate Victoria Stempniewicz, Andrew Gray, James Guilinger, and the rest of the United States Forest Service hydrologists and UC Riverside researchers in attendance at the 2020 Holy Fire Research Symposium for sharing updates on the recovery. Finally, we appreciate Brian Swanson (Department of Conservation - California Geological Survey) for sharing his observations and findings following the 2018 Holy Fire. We also appreciate Jason Uhley and multiple support staff at the Riverside County Flood Control and Water Conservation District, and local residents including Dale Hook, Peter Rasinski, Shannon Akins, and Sue Engelhardt for sharing observations and findings following the 2018 Holy Fire. Last but not least, the authors of this work would also like to acknowledge that data for areas affected by the 1980 Dry Falls Fire, the 2000 Pechanga Fire, and the 2013 Mountain Fire came from lands belonging to the Pechanga Band of Luiseño Indians and the Agua Caliente Band of Cahuilla Indians. We recognize the continuing and long-lasting presence of all indigenous groups of this land.

Table of Contents

List of Abbreviations/Acronyms, Keywords.....	1
Abstract.....	2
Acknowledgements	3
Table of Contents	4
List of Figures.....	5
List of Tables.....	6
1. Objectives.....	1
2. Background.....	1
3. Materials and Methods	2
3.1 RCS Evaluation and Machine Learning Peak flow Model.....	4
3.2 Spatial and Temporal Ecohydrological Analysis.....	4
4. Results and Discussion	4
4.1 RCS Evaluation and Machine Learning Peak Flow Model.....	4
4.2 Vegetation Production for the 2018 Holy Fire Site	9
4.3 Science Delivery Activities	15
5. Key Findings and Implications for Policy and Future Research.....	16
6. Literature Cited.....	18
Appendix A: Contact Information for Key Project Personnel	28
Appendix B: List of Science Delivery Products.....	29
Appendix C: Metadata.....	30

List of Figures

Figure 1. Percent of county area burned in California from 2000 to 2020 (data source: Moderate Resolution Imaging Spectroradiometer Burned Area Monthly Global at 500-m). Study area shown in the dashed black rectangle.	2
Figure 2. Study area consisted of 33 watersheds in 6 different regions within the Transverse Ranges and Peninsular Ranges in southern California, USA. The 2018 Holy Fire is noted by a red oval.	3
Figure 3. Rowe, Countryman, and Storey (RCS) unburned peak streamflow predictions compared to observed peak streamflow for 2-year (A) and 10-year (B) return periods.	5
Figure 4. Predictions for the five parameter random forest (RF-5) model by region. The sample size (n) is noted for each region.	7
Figure 5. Observed peak streamflow versus predicted streamflow response. The black line represents a perfect prediction. Squares represent RCS (2- and 10-year events) and triangles represent random forest with the five most important parameters (RF-5). RF-5 is based on the entire training dataset and has no affiliated event magnitude. The extreme conditions or the highest floods for each watershed are shown (n = 33).	7
Figure 6. Observed peak streamflow per unit area with respect to peak hourly rainfall intensities (a), watershed size (b), and days after fire containment (c).	9
Figure 7. Standardized Precipitation Index (SPI) for WY 1991 to 2020 and annual ET_{SSEBop} for WY 2001 to 2020 for the area affected by the Holy Fire. The approximate date of the fire is denoted by a vertical dashed line.	10
Figure 8. Pre-fire ΣEVI (WY 2014 to 2017) with respect to soil burn severity in the Holy Fire, where n represents number of EVI pixels. The proportion of soil burn severity for each of the vegetation types are shown on the secondary axis.	11
Figure 9. Spatial representation of ET_{PT-JPL} and ET_{SSEBop} pre-fire on August 2, 2018 (a and b), one year after fire on August 17, 2019 (d and e), and two years after fire on October 3, 2020 (g and h). Correlations between ET_{PT-JPL} and ET_{SSEBop} (n = 103 pixels) (c, f, and i) include a regression line and shading, which represents the standard error.	12
Figure 10. Daily rainfall (a), difference in daily evapotranspiration (ΔET) from WY 2019 to 2020 (b), and Coldwater and Santiago daily streamflow (c). The difference in ECOSTRESS PT-JPL ET (ΔET_{PT-JPL}) is Santiago (unburned) minus Coldwater (burned). The dashed green line represents a 60 day rolling average of ΔET_{PT-JPL}	13

List of Tables

Table 1. Originally proposed objectives and projected delivery dates (check marked if completed)	1
Table 2. Cumulative ET_{PT-JPL} (ΣET) from WY 2019 (25 images) and WY 2020 (48 images) for the Holy Fire with respect to riparian versus hillslope, soil burn severity, slope aspect, and pre-fire vegetation species.	14

1. Objectives

The primary objectives of this study (Table 1), were to identify knowledge gaps in post-fire watershed models and improve the performance of a widely used post-fire peak flow prediction tool (Wilder et al., 2021). Additionally, we characterized pre-fire vegetation conditions and post-fire vegetation recovery after the 2018 Holy Fire using high resolution satellite products (Wilder & Kinoshita, in review).

Table 1. Originally proposed objectives and projected delivery dates (check marked if completed)

Project Milestone	Description	Delivery Dates	
Phase 1	Watershed Characterization and Analysis	Sep 2019	✓
Phase 2 (Task 1)	Model Evaluation – Uncertainty and Errors	Mar 2020	✓
Phase 2 (Task 2 and 3)	Model Evaluation – Explanatory Variables and Calibration	Dec 2020	✓
Phase 3	Improve Peak Flow Estimate Methods	May 2021	✓
M.S. Thesis	Journal Manuscript, Thesis Defense, and data submission	Aug 2021	✓

2. Background

Fire frequency and severity in California, and across the western United States, are increasing (Steel et al., 2015). Increased aridity coupled with decades of fire suppression and water stressed vegetation from prolonged droughts are leading to a higher propensity for larger and more intense fires that directly impact ecohydrological processes. Accurate characterization of these processes will improve rapid response efforts and long-term resource management to promote resilient communities along the wildland-urban interface.

Across the State of California, the percent county area burned (proportion of total burned area in relation to county area) ranged from 0-65% over the past 20 years (Figure 1). While some counties in northern California had proportions of burned area that were over 50%, this work focuses on understanding the impacts of wildfire in southern California which has had some of the most destructive fires in the state (CAL FIRE, 2021). High proportions of total wildfire area in southern California from 2000 to 2020, include Ventura County (50%), San Diego County (37%), Los Angeles County (28%), Santa Barbara County (22%), and Orange County (15%). These frequent fires can change the post-fire landscape, producing elevated peak streamflows in small watersheds (Neary et al., 2005) and variant (spatially and temporally) ecohydrological recovery (Kinoshita & Hogue, 2011). Under changing climate and wildfire regimes, accurate predictions of post-fire peak streamflow rates and ecohydrological recovery are critical for key emergency response and management agencies such as the California Department of Forestry and Fire Protection (CAL FIRE), California Department of Conservation – California Geological Survey (CGS), the U.S. Forest Service (USFS), and local county flood control districts who seek to mitigate risks associated with post-fire flooding and erosion. Further, long-term vegetation assessments are essential for planning and informing recreational infrastructure such as trail and road access to the public.

Models used to predict post-fire hydrologic processes have varying degrees of sophistication (Atchley et al., 2018; Cannon et al., 2004; Kinoshita et al., 2014; Robichaud et al., 2007; Wilder et al., 2021). Due to the short time period between fire and flood in southern California, simpler flood frequency models such as Rowe et al. (1949) are prioritized to rapidly

assess risks to downstream communities and ecosystems (Kinoshita et al., 2014; Wilder et al., 2021). Thus, this research investigates methodologies to improve prediction tools for rapid and long-term risk assessments for downstream communities and ecosystems. We demonstrate how machine learning methods can be implemented into assessments immediately after fire. We also incorporate a case study to estimate annual water yield in semi-arid sites for small, burned watersheds and close the water balance for fire-prone landscapes.

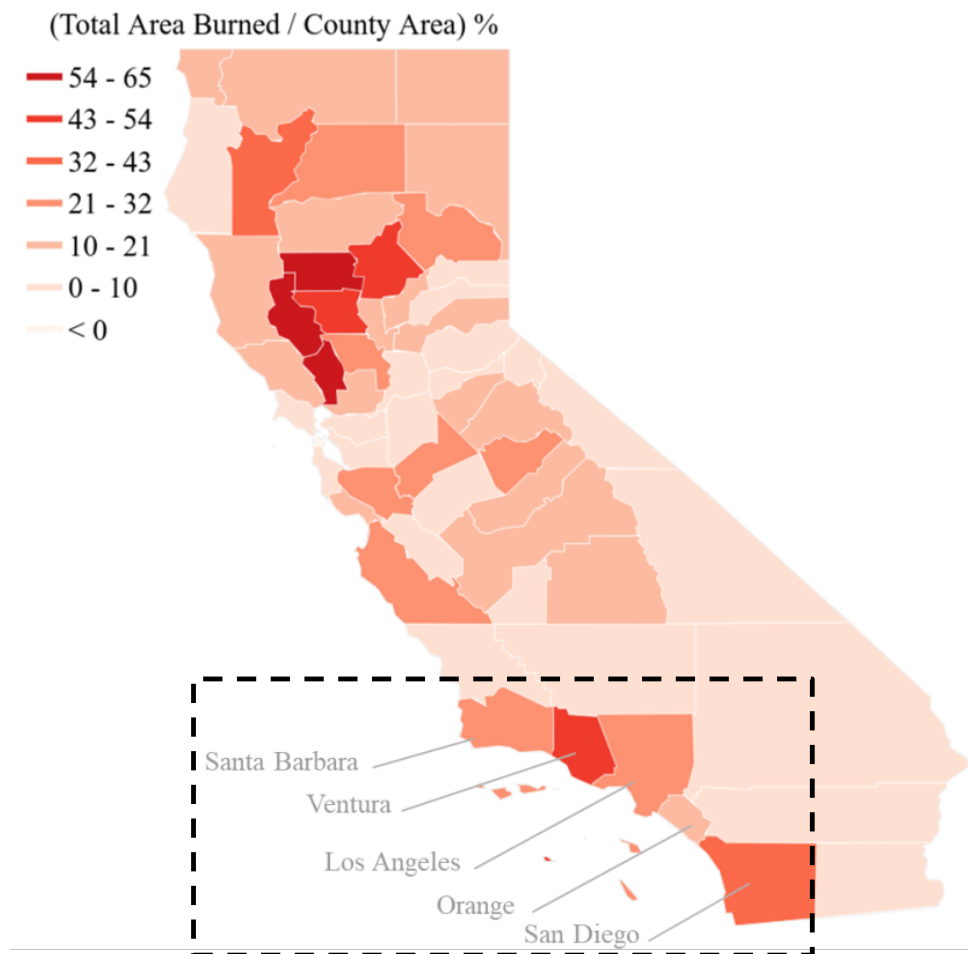


Figure 1. Percent of county area burned in California from 2000 to 2020 (data source: Moderate Resolution Imaging Spectroradiometer Burned Area Monthly Global at 500-m). Study area shown in the dashed black rectangle.

3. Materials and Methods

The study area is within the Transverse Ranges and Peninsular Ranges, which are geomorphic provinces with a wide topographic range from sea level to 3506 m (CGS, 2002). The study area straddles the southern California Coastal and southern California Mountain and Valleys ecoregions (Cleland et al., 2007). Approximately 60%–70% of these ecoregions are dominated by shrubland (e.g., chaparral) vegetation types, with a lesser proportion occupied by grassland and woodland or forest vegetation types (FRAP, 2015). The median presettlement fire

return intervals for these vegetation types are variable, ranging on average from approximately 60 to 100 years for chaparral and coastal scrub vegetation types (Van de Water & Safford, 2011).

This research focused on 33 small watersheds with drainage areas ranging between 1.2 to 41.7 km² (Figure 2) to address the primary objective of this study: to identify knowledge gaps in post-fire watershed models and improve the performance of a widely used post-fire peak flow prediction tool (Section 3.1). Additionally, we characterized pre-fire vegetation conditions and post-fire vegetation recovery after the 2018 Holy Fire using satellite products (Section 3.2). The Holy Fire occurred in the Santa Ana Mountains in early August of 2018 (Figure 2) and burned approximately 94 km². The soil burn severity classifications for the Holy Fire were approximately 14% high, 71% moderate, 8% low, and 7% low to unburned (WERT, 2018). It is noted that the 2020 Bond Fire burned the foothills approximately 20 km northwest of the Holy Fire. The Bond Fire occurred almost entirely outside of the study area and after the study period, thus minimally impacting our analysis.

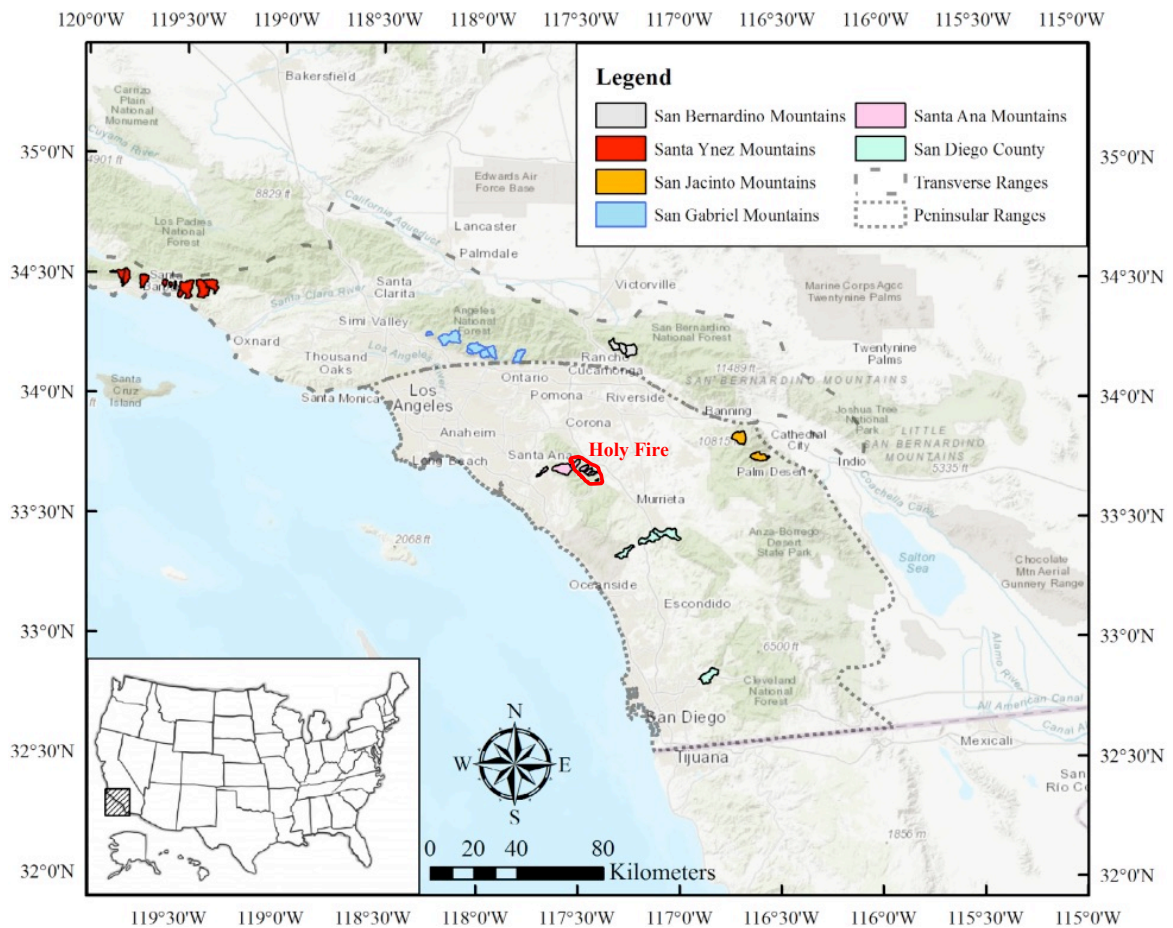


Figure 2. Study area consisted of 33 watersheds in 6 different regions within the Transverse Ranges and Peninsular Ranges in southern California, USA. The 2018 Holy Fire is noted by a red oval.

3.1 RCS Evaluation and Machine Learning Peak flow Model

Post-fire peak flow observations for the 33 study watersheds were acquired from the USGS for the study period between 1920 to 2019 (Wilder et al., 2021). The flood recurrence intervals for peak flow observations were computed by the Weibull and USGS PeakFQ methods (Clarke, 2002; Flynn et al., 2006) and the two methods were averaged to form baseline peak flow observations for each watershed. A regression analysis was used to compare the pre- and post-fire baseline observations to the RCS 1949 (Rowe et al. (1949)) flood frequency methodology. Correlation (R^2), root mean squared error (RMSE), standard deviation, and bias were calculated to assess performance of 2- and 10-year recurrence interval predictions, the most used recurrence intervals for flood prediction in southern California.

We developed a flood forecasting, machine learning (random forest) algorithm using hydrological and meteorological input data provided by new information and technologies. The inputs of this model were formulated by aggregating 45 unique watershed parameters based on an extensive post-fire literature review. We identified important factors that represented realistic conditions and increased accuracy of the random forest predictions, which were used to develop a random forest with five unique watershed parameters (RF-5). Our developed model predicted post-fire peak flow rates for small watersheds (Wilder et al., 2021).

3.2 Spatial and Temporal Ecohydrological Analysis

Building upon previous studies (i.e., Poon & Kinoshita, 2018), we incorporated ET at improved resolution to assess disturbance from fire in small watersheds (Wilder & Kinoshita, in review). Local rainfall and runoff data were used to calculate hydrologic signatures (McMillan, 2020) at the annual timescale to quantify changes in streamflow, water balance, and recovery based on a paired watershed approach. These metrics were calculated for Santiago and Coldwater for WY 2014 to 2020 for all available streamflow data. Additional data were collected including ECOSystem Spaceborne Thermal Radiometer Experiment on Space Station (ECOSTRESS) Priestley-Taylor Jet Propulsion Laboratory Algorithm (PT-JPL) ET (ET_{PT-JPL}), Operational Simplified Surface Energy Balance Model (SSEBop) ET (ET_{SSEBop}), satellite-based annual vegetation biomass accumulation using summation of Enhanced Vegetation Index (ΣEVI), vegetation species types using CAL FIRE Fveg database, and soil burn severity classifications. Spatial datasets were analyzed in Google Earth Engine and differentiated with respect to slope aspect, pre-fire vegetation species, riparian versus hillslope, and soil burn severity classifications.

4. Results and Discussion

4.1 RCS Evaluation and Machine Learning Peak Flow Model

We compared the pre-fire predictions with the baseline observed data normalized by the watershed area (Figure 3). In total, the pre-fire 2-year return period had a positive bias of 0.162 cms/km² and the 10-year return period had a negative bias of -0.791 cms/km². There was also substantial error in RMSE and variation in standard deviation that RCS 1949 did not represent. For example, the standard deviation for the RCS 10-year return period was 0.31 cms/km², while the standard deviation of the observed 10-year return period was 1.28 cms/km². The Santa Ynez region had the lowest accuracy by region for the 10-year return period, bias = -2.362 cms/km², and Franklin Canyon, within the Santa Ynez region, had the lowest accuracy for all watersheds, where 10-year return period peak flow was under-predicted by a factor of 4.75. Overall, pre-fire peak streamflow prediction performance was low for the 2- and 10-year recurrence interval

events ($R^2 = 0.24$ and $RMSE = 0.38$ cms/km²; $R^2 = 0.34$ and $RMSE = 1.43$ cms/km², respectively).

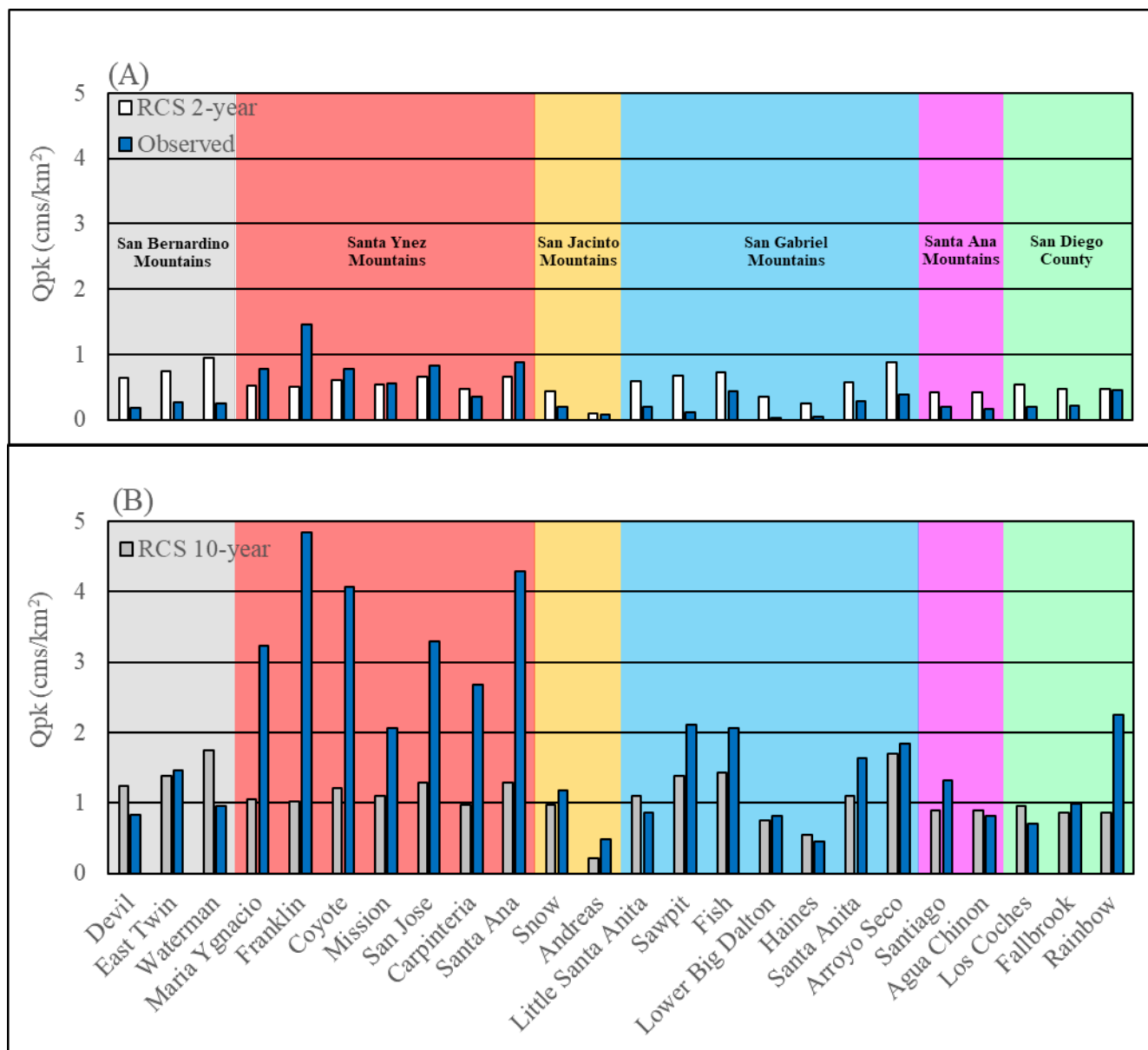


Figure 3. Rowe, Countryman, and Storey (RCS) unburned peak streamflow predictions compared to observed peak streamflow for 2-year (A) and 10-year (B) return periods.

Based on post-fire observed flow, 22 watersheds experienced flooding that were under predicted by the RCS 10 year predictions during the first five years after fire. Observed post-fire flows were compared to the probabilistic predictions, yielding R^2 and RMSE for RCS 2-year return periods of 0.26 and 16.01 cms/km², and R^2 and RMSE for RCS 10-year return periods of 0.25 and 15.52 cms/km², respectively. Predictions generally had large negative bias with 2-year return periods yielding -8.68 cms/km² and 10-year return periods yielding -7.78 cms/km².

Regionally, 13 watersheds observed post-fire peak streamflow rates larger than the RCS 100-year prediction. Watersheds in the San Diego and San Jacinto regions had on average 149% lower post-fire peak streamflows compared to the other regions. Predictions for watersheds in the Santa Ynez, San Gabriel, San Bernardino, and Santa Ana mountains were inaccurate, with errors ranging up to 1720% during the floods at Dickey Canyon after the 2018 Holy Fire. These flows were rapid, where field observed velocity was measured to be approximately 12 m/s (B. Swanson, personal communication, October 2019).

In general, RCS 1949 demonstrated large inaccuracy for small watersheds (1 to 42 km²). This is attributed to a multitude of factors including watershed morphology, exclusion of soil burn severity, greater development in the wildland urban interface, and increasing frequency in extreme weather events due to climate change since the development of this model. The largest inaccuracies were observed for watersheds in the Santa Ynez Mountains, which is of concern due to the tendency for hazardous events in this region, such as the January 9, 2018 Montecito debris flows (Kean et al., 2019). Clear water flows generally have suspended-sediment concentrations of less than 5% to 10% sediment by volume, while hyperconcentrated flows and debris flows can have suspended-sediment concentrations from 5% to 60% and >60% sediment by volume, respectively (Pierson, 2005). The RCS 1949 regressions were developed for flows with low sediment concentrations (non-bulked flows); therefore, RCS predictions are expected to be limited and unable to predict peak flows associated with debris flows. Accurate predictions of post-fire streamflow along the continuum from flooding to debris flows are needed due to their frequent occurrence following wildfire in southern California (Cannon & DeGraff, 2009).

Our results highlight the need to incorporate the significant advances in post-fire hydrology since the development of Rowe et al. (1949) to improve the accuracy of predictions (Wilder et al., 2021). For example, sediment bulking is implicit in RCS, yet independent variables that are strongly linked to sediment production or sediment yield are not used. Additionally, this observation-based method predates the development of the soil burn severity metric. Soil burn severity characterizes the fire-induced changes in soil and ground cover properties that can affect infiltration, runoff, and erosion potential (Parsons et al., 2010) and is incorporated in post-fire hydrogeomorphic modelling as an independent variable to predict debris flows and debris yield (Gartner et al., 2014; Staley et al., 2017).

A random forest machine learning algorithm with 45 watershed parameters (RF-45) was created with meteorological and watershed properties to predict post-fire peak streamflow for 1920 to 2019. The time elapsed after fire, peak hourly rainfall intensity, and drainage area were important factors that represented realistic conditions and increased accuracy of the random forest predictions and were represented in the RF-5 model (RF-5 contained five most important parameters). The RF-5 model ($R^2 = 0.46$ and $RMSE = 7.89$ cms/km²) performed better than the RCS method and was better able to capture the extreme variability of post-fire peak flows (Figure 4). This is exemplified by the model sensitivity to the extreme post-fire responses for the 33 highest magnitude post-fire storm events for each of the study watersheds (Figure 5). The RCS 2-year and RCS 10-year RMSE values were 16.01 cms/km² and 15.52 cms/km², respectively, while the random forest machine learning model RMSE was lower at 10.41 cms/km².

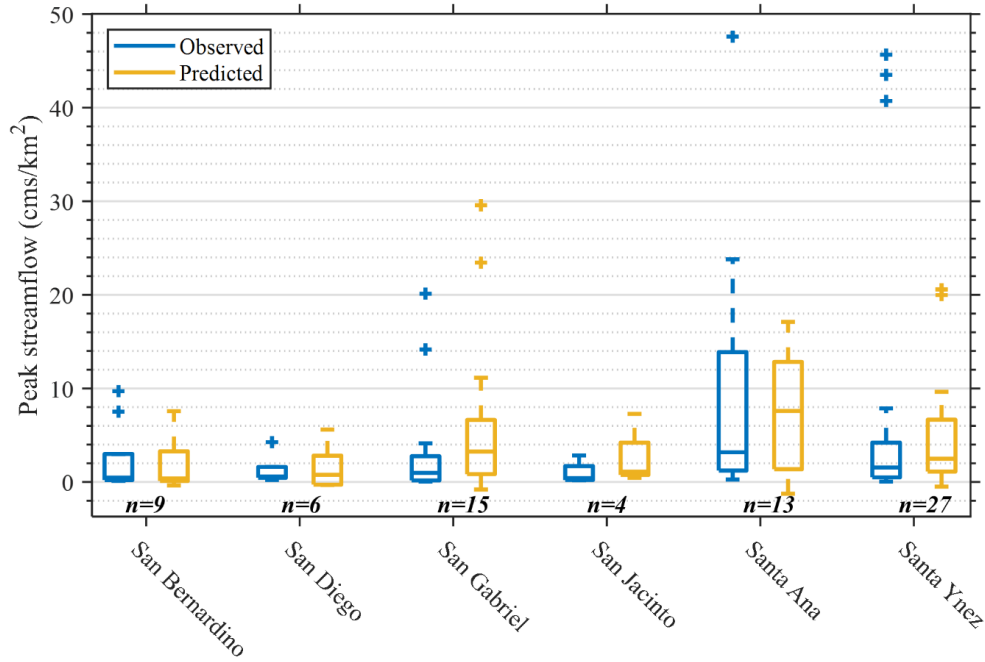


Figure 4. Predictions for the five parameter random forest (RF-5) model by region. The sample size (n) is noted for each region.

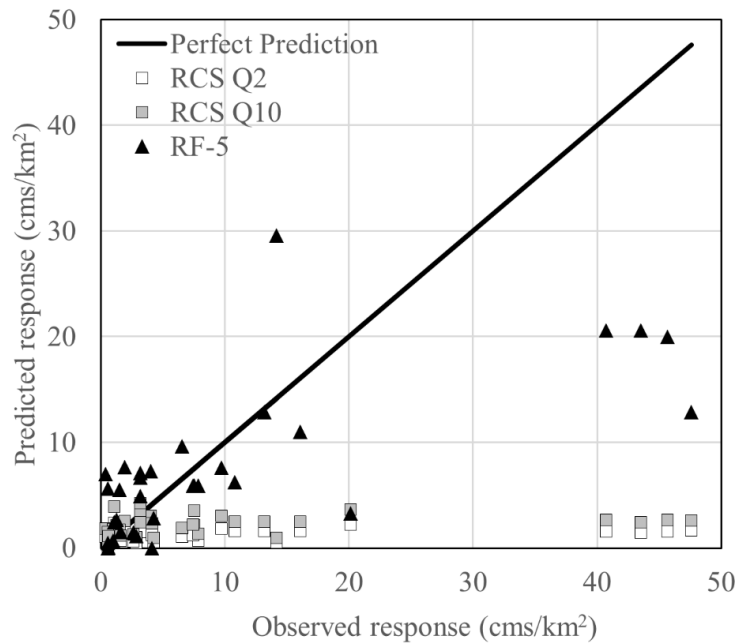


Figure 5. Observed peak streamflow versus predicted streamflow response. The black line represents a perfect prediction. Squares represent RCS (2- and 10-year events) and triangles represent random forest with the five most important parameters (RF-5). RF-5 is based on the entire training dataset and has no affiliated event magnitude. The extreme conditions or the highest floods for each watershed are shown (n = 33).

Our findings from the machine learning approach agreed with previous studies. For example, peak hourly rainfall intensities over 10 mm/h led to larger magnitude floods (Figure 6a). These results are attributed to physical watershed processes, whereby larger peak rainfall intensities increase rill erosion and channel incision (Cannon & DeGraff, 2009). Watersheds with smaller areas (1–10 km²) were more likely to have larger magnitude runoff per unit area ($p < 0.05$) (Figure 6b). Our observations are similar to Neary et al. (2005), who reported much larger magnitudes (average post-fire peak flows of 193 cms/km²) for very small watersheds in Western United States (<1 km²). Further, in smaller watersheds with predominantly chaparral vegetation, runoff responses can be erratic and have potential to transport large amounts of sediment per unit area after fire (Keller et al., 1997), highlighting the increased potential for higher magnitude peak flows. Finally, storms that occurred closer in time to the containment of the fire had a higher likelihood of larger magnitude events ($p < 0.05$) (Figure 6c). The passing of time allows hydrophobic soils to normalize and vegetation to recover, reducing rainfall impact on bare soil (Neary et al., 2005).

The most important parameters identified by machine learning were time after fire (to distinguish events within the first year), rainfall intensity, and burned area and used to create a simple regression. Thirty-one rainfall-runoff events during the first year after fire from the study area were fitted to a three-dimensional polynomial function ($R^2 = 0.82$):

$$Qpk = -8.316 + 0.4033(A) + 0.9041(i60) - 0.04079(A)(i60) + 0.0127(i60)^2 \quad (1)$$

where Qpk is peak streamflow (cms/km²), A is burned area (km²), and i60 is peak hourly rainfall intensity (mm/h). Watershed area and watershed perimeter were not used for the regression. On average, burn proportions consisted of 56% moderate to high soil burn severity and 44% unburned to low soil burn severity.

Machine learning requires data collection, calibration, and parameterization that should be carried out cautiously. Excluding or missing parameters that have significant importance to model accuracy can lead to highly inaccurate predictions due to insufficient processes being defined by the data. Nevertheless, our study demonstrates that with enough high-quality data, machine learning can be a valuable procedure for developing predictive tools for post-fire risk assessment.

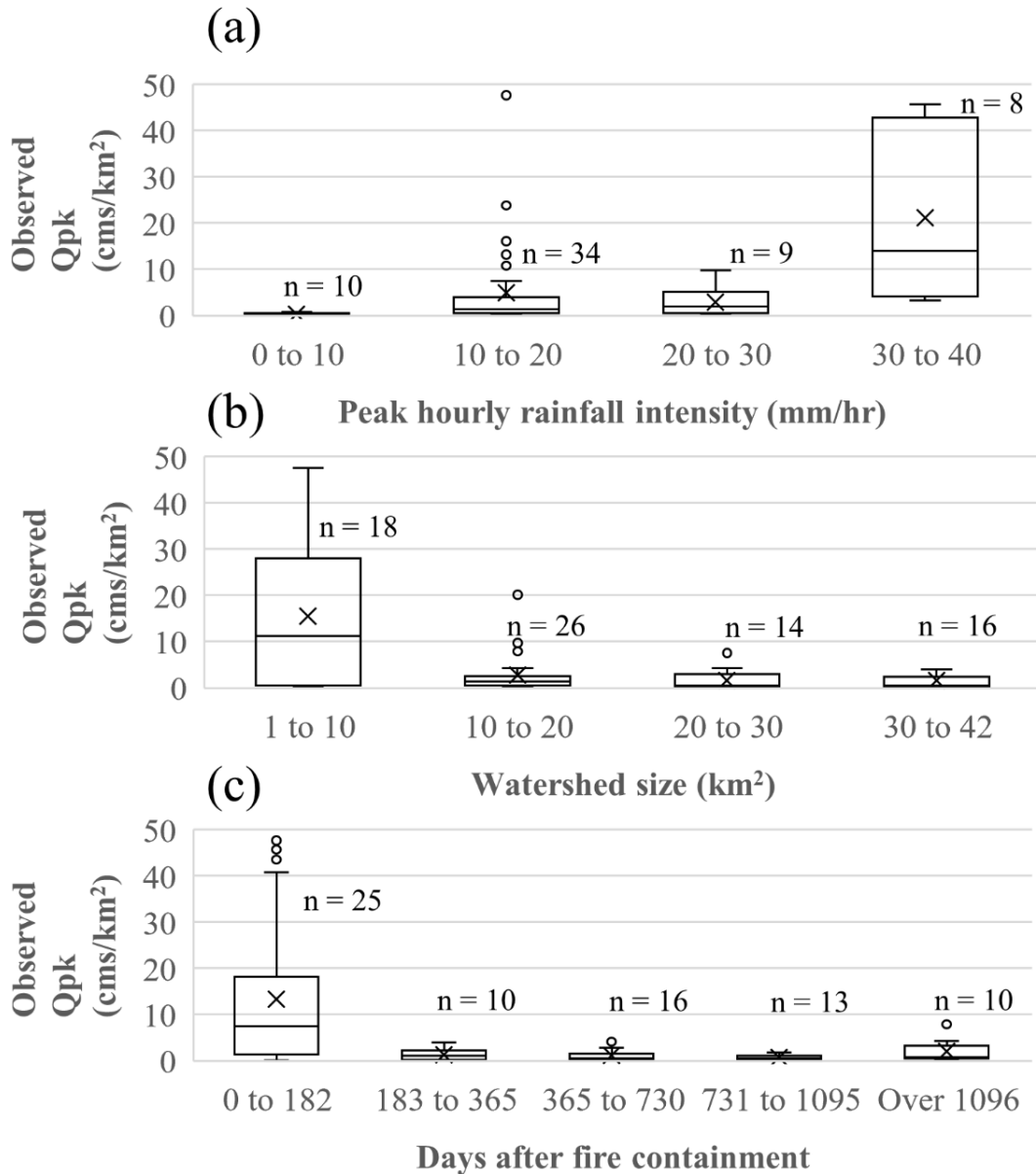


Figure 6. Observed peak streamflow per unit area with respect to peak hourly rainfall intensities (a), watershed size (b), and days after fire containment (c).

4.2 Vegetation Production for the 2018 Holy Fire Site

Annual SPI (WY 1991 to 2020) and ET_{SSEBop} (WY 2001 to 2020) were calculated for the Holy Fire burn scar (Figure 7). Wet years appeared intermittently, typically after four to six moderately dry to normal years. No years had an SPI greater than 1.0 in 2012 to 2018 (no wet years), highlighting the seven year drought period prior to the fire. This extended dry period is documented as an extreme drought that caused widespread plant stress across northern and southern California (Dong et al., 2019). Water year 2019 was a moderately wet year that followed the Holy Fire (SPI = 1.17). This year had several intense storms, with 15-minute rainfall intensities as high as 32 mm/hr (Guilinger et al., 2020).

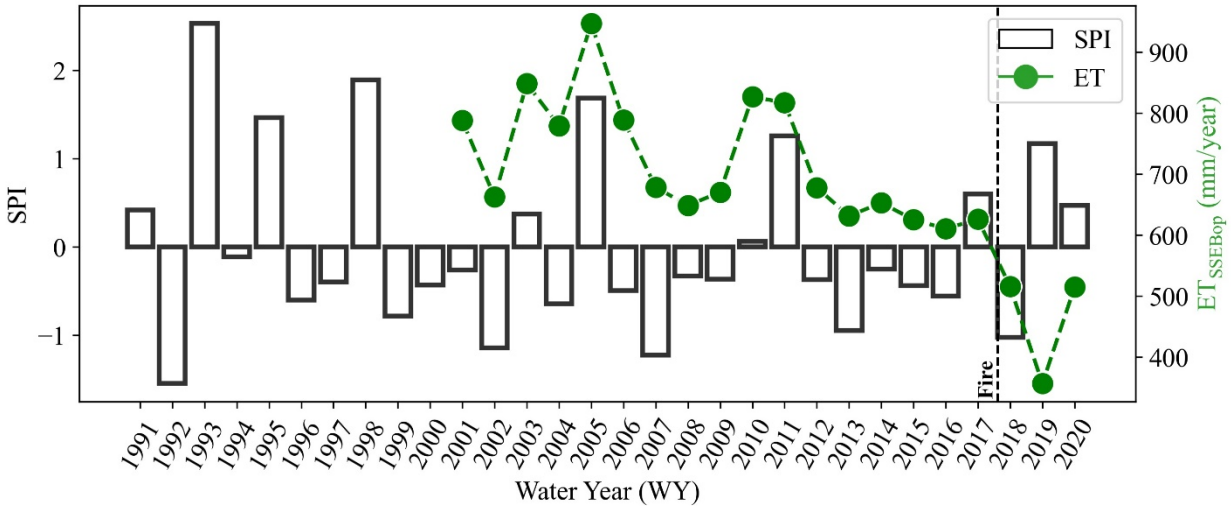


Figure 7. Standardized Precipitation Index (SPI) for WY 1991 to 2020 and annual ET_{SSEBop} for WY 2001 to 2020 for the area affected by the Holy Fire. The approximate date of the fire is denoted by a vertical dashed line.

From WY 2001 to 2017, the average annual pre-fire ET_{SSEBop} was 722 mm for the entire area and ranged from 610 to 947 mm. The three years prior to the fire had the lowest ET, ranging from 610 to 625 mm. Additionally, all seven years prior to the fire were below the pre-fire average. A modest correlation existed between pre-fire annual ET and SPI ($R^2 = 0.41$; $n = 17$), where generally the extreme wet and dry years had relatively high ET (i.e., 947 mm in WY 2005) and low ET (i.e., 678 mm in WY 2007), respectively. After the fire in 2019, there was 1,036 mm of rainfall, resulting in a large resurgence in ET (44% increase) in WY 2020. Focusing on the seven year drought period (WY 2012 to 2018; note that 2018 only includes August and September prior to the fire), we compared the monthly ET_{SSEBop} to the eleven years prior to the drought (WY 2001-2011). This period encompassed typical cyclical climate fluctuations (two moderately wet years, two moderately dry years, and seven normal years) associated with El Niño-Southern Oscillation patterns. The two time periods were statistically different ($p < 0.05$) for all months (except for November), where the seven year drought before the fire had significantly lower ET. During the pre-fire period (WY 2001 to 2017), monthly ET typically peaked in the dry season between June to July, with values ranging from 64 to 151 mm/month. Most notably, one month prior to the fire in WY 2018, the observed ET had the lowest July monthly value of 64 mm/month.

The prolonged drought had a significant impact on montane hardwood species and other areas, making these areas more prone to high soil burn severity (Figure 8). Areas with larger pre-fire ΣEVI , ranging from 14 to 16, were associated with high soil burn severity ($p < 0.05$). In particular, montane hardwood species had the greatest proportion of high soil burn severity for all vegetation types, where 33% of this vegetation type burned at high severity. We hypothesize that the severe seven year drought prior to the fire increased water stress and fuel load in the montane hardwood species in the Holy Fire area, explaining the increased severity observed (Guarín & Taylor, 2005). While ECOSTRESS was not available prior to the fire (launched in June 2018), we advocate that ET and ESI (evaporative stress index) can be important tools for

future assessments of water stress and potential fire risk.

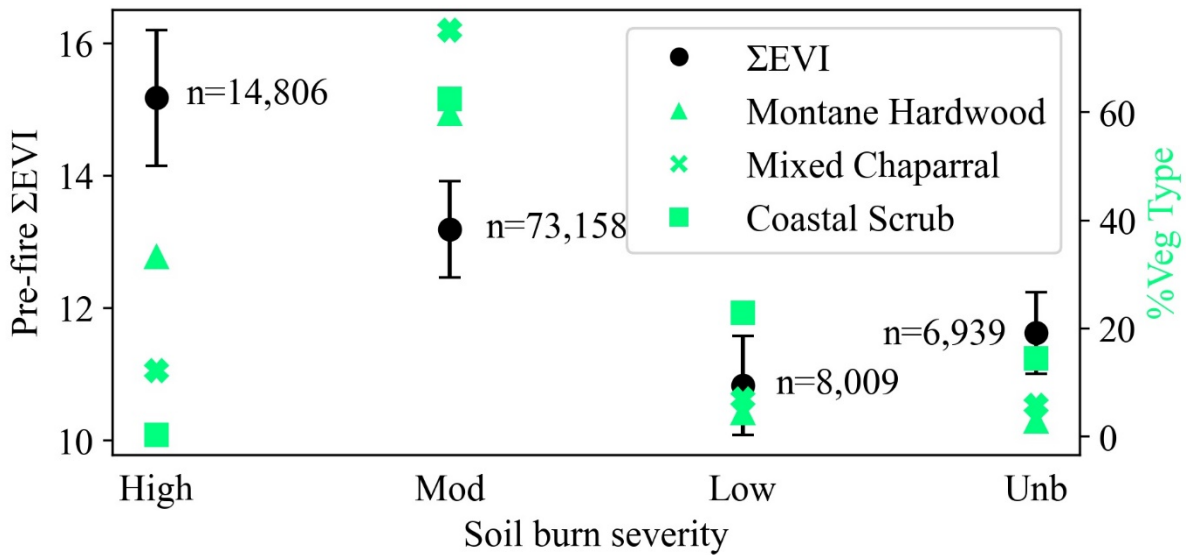


Figure 8. Pre-fire Σ EVI (WY 2014 to 2017) with respect to soil burn severity in the Holy Fire, where n represents number of EVI pixels. The proportion of soil burn severity for each of the vegetation types are shown on the secondary axis.

We examined the variability of the remotely sensed ET throughout the burned landscape. ET_{SSEBop} and ET_{PT-JPL} images before and after the Holy Fire were compared and resulted in comparatively higher variability between the two ET products after the fire (Figure 9). The pre-fire R^2 was 0.47, while post-fire R^2 ranged from 0.00 to 0.04. The pre-fire slope of the linear regression between the two datasets was 0.36 (Figure 9c). The range decreased post-fire to values between -0.10 to 0.12 and the standard error of the regression line was generally larger for the post-fire images (Figures 9f and 9i). The large variability observed between ET_{SSEBop} and ET_{PT-JPL} for both post-fire years were likely due to the inherent and complex spatial heterogeneity of the burned conditions. This can lead to sub-pixel contamination of the SSEBop pixels for the sensitive inputs such as land surface temperature and reference ET (Chen et al., 2016). SSEBop at 1 km spatial resolution may not be suitable for capturing fine-scale post-fire processes of semi-arid and dry regions and is noted by Chen et al. (2016) to be most reliable for large-area estimates of ET. The smaller footprint of ET_{PT-JPL} better captures spatial heterogeneity present in post-fire parameters such as land surface temperature and reference ET.

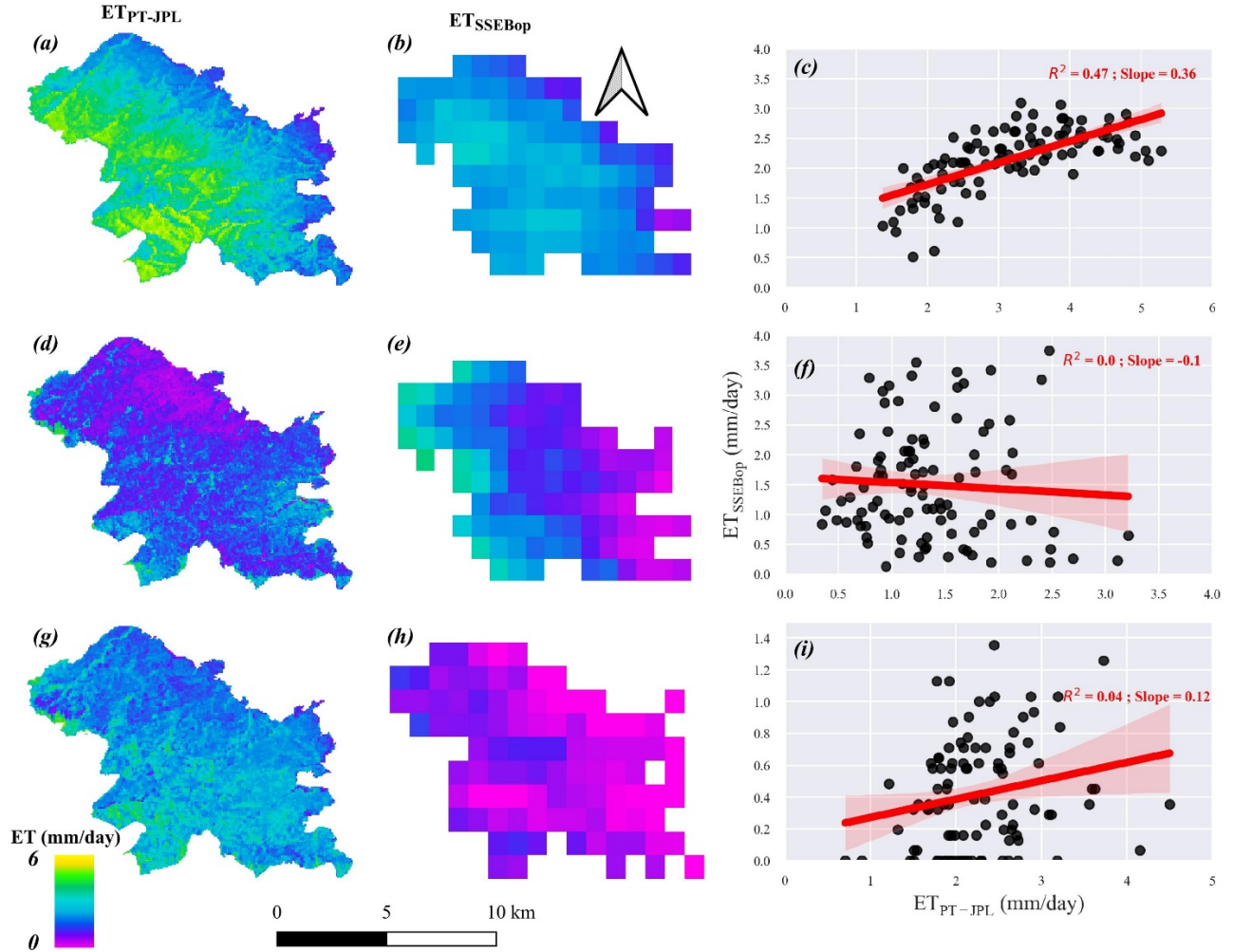


Figure 9. Spatial representation of ET_{PT-JPL} and ET_{SSEBop} pre-fire on August 2, 2018 (a and b), one year after fire on August 17, 2019 (d and e), and two years after fire on October 3, 2020 (g and h). Correlations between ET_{PT-JPL} and ET_{SSEBop} ($n = 103$ pixels) (c, f, and i) include a regression line and shading, which represents the standard error.

Additionally, rainfall from the Upper Silverado rainfall station, difference in ET between the two watersheds (ΔET_{PT-JPL}), and runoff between the two watersheds for WY 2019 to 2020 highlighted seasonal patterns in the post-fire recovery (Figure 10). The burned watershed had comparatively higher magnitude of runoff in the winter months and reduced ET in the summer months. ET differences between the two watersheds were highly sinusoidal after the fire. The largest difference in magnitude (2 to 3 mm) between the unburned and burned watersheds was in the dry months and the smallest difference (0 to 1 mm) was during the wet months. In general, based on ET_{PT-JPL} measurements, the burned watershed produced less ET during the post-fire study period than the unburned watershed for all seasons. This supported the findings of previous studies, which have noted decreased post-fire ET in semi-arid regions (Poon & Kinoshita, 2018; Prater & DeLucia, 2006; Ma et al., 2020; Nolan et al. 2014; Soulis et al., 2021).

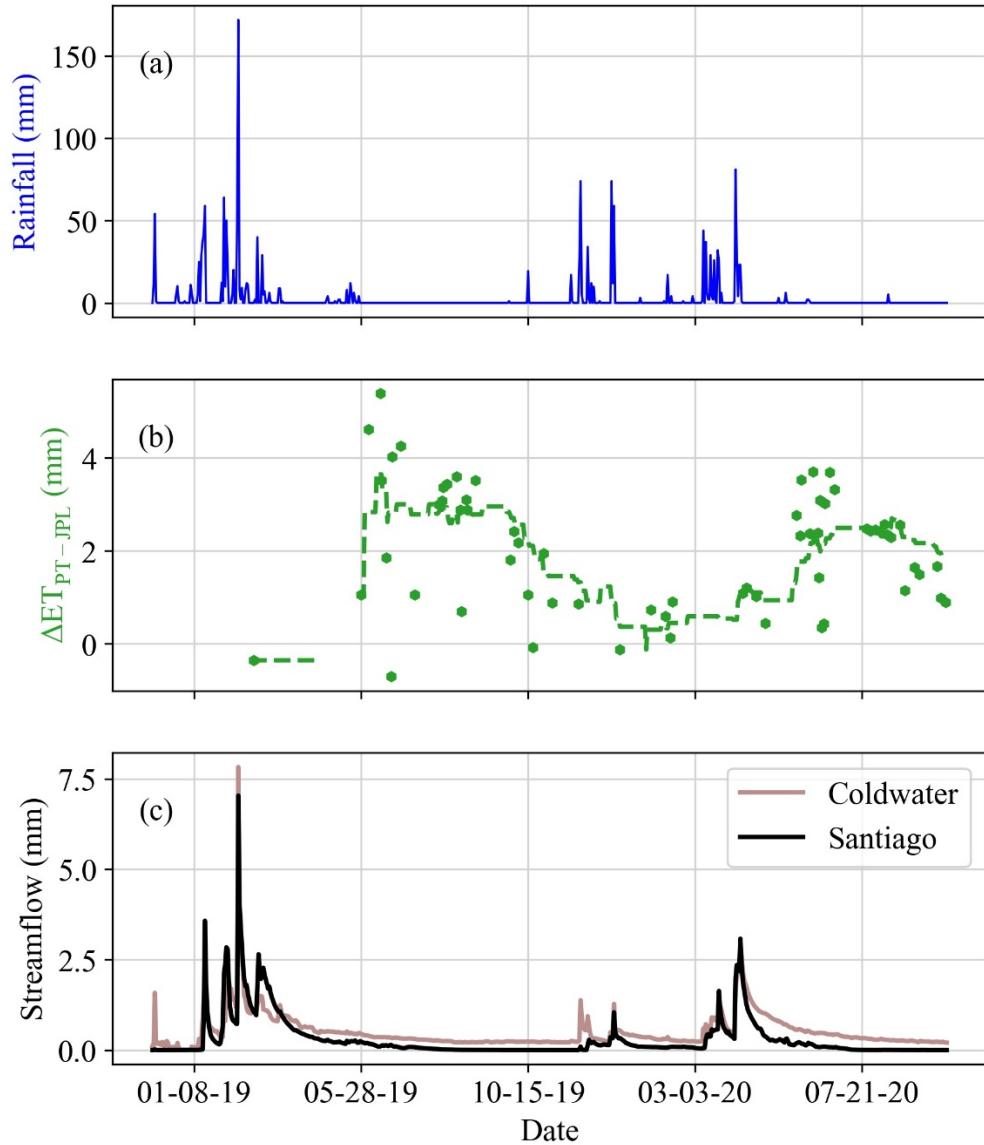


Figure 10. Daily rainfall (a), difference in daily evapotranspiration (ΔET) from WY 2019 to 2020 (b), and Coldwater and Santiago daily streamflow (c). The difference in ECOSTRESS PT-JPL ET (ΔET_{PT-JPL}) is Santiago (unburned) minus Coldwater (burned). The dashed green line represents a 60 day rolling average of ΔET_{PT-JPL} .

Cumulative ET_{PT-JPL} collected from February 2019 to October 2020 (73 images) varied with respect to landscape subgroups: slope aspect, soil burn severity, riparian/hillslope, and pre-fire vegetation species (Table 2). ET production was homogeneous across the landscape subgroups during the first year after fire. Most notably for WY 2019, the montane hardwood species in higher elevations had the largest ΣET for the first year after fire. In WY 2019, the ET and EVI varied minimally by slope aspects, burn severity, and riparian areas (± 2 mm from the mean), suggesting relatively homogeneous conditions across the burned landscape. Differences in the ET production across the landscape subgroups was not observed until the second year after

fire. In WY 2020, areas with pre-fire montane hardwood species had the highest ET production (297 mm) out of all the vegetation species. Also for WY 2020, high burn severity areas had the second largest ET production (296 mm) out of all the subgroups and areas of west facing slopes had the third highest ET production (294 mm).

Table 2. Cumulative ET_{PT-JPL} (ΣET) from WY 2019 (25 images) and WY 2020 (48 images) for the Holy Fire with respect to riparian versus hillslope, soil burn severity, slope aspect, and pre-fire vegetation species.

Landscape sub-groups	WY 2019 ΣET (mm)	WY 2020 ΣET (mm)
Riparian (n=1,205)	118	283
Outside of riparian (n=17,979)	120	289
High (n=2,743)	120	296
Moderate (n=13,563)	119	289
Low (n=1,477)	120	272
North (n=7,014)	121	290
East (n=5,019)	119	284
South (n=4,251)	119	289
West (n=2,900)	122	294
Mixed Chaparral (n=12,878)	120	290
Montane Hardwood (n=3,000)	124	297
Coastal Scrub (n=1,038)	110	261
<i>Mean for the burned area</i>	<i>120</i>	<i>287</i>
<i>Standard Deviation for the burned area</i>	<i>5</i>	<i>11</i>

Post-fire ET_{PT-JPL} data appeared to represent the conditions of the Holy Fire and were similar to other studies that documented decreases in post-fire ET (Poon & Kinoshita, 2018; Prater & DeLucia, 2006; Ma et al., 2020; Nolan et al. 2014; Soulis et al., 2021). However, more work needs to be done to field validate ET_{PT-JPL} in post-fire settings across diverse ecoregions and longer timespans. Along with ground-based validation efforts, the use of Unmanned Aircraft Systems (UAS) may present an opportunity to improve certainty in post-fire assessments of satellite-based ET (Fernández-Guisuraga et al., 2018). Additionally, soil moisture was not within the scope of this work, however, future studies are encouraged to integrate field observations and measurements of soil moisture to provide further insight into the water balance and storage dynamics for burned catchments. While this study is a preliminary presentation of ECOSTRESS,

we advocate that high spatial and temporal resolution data will supplement and aid in answering crucial science questions for future fires. For example, like Poon & Kinoshita (2018), we identified general patterns during our study period using a lower resolution SSEBop product. However, ECOSTRESS provides scientists with higher resolution tools (i.e., ET and Evaporative Stress Index products) that can be used to improve precision for fire analysis. In the case of the Holy Fire, areas such as the montane hardwoods that burned at high soil burn severity can be evaluated by scientists to understand pre-fire water stress and dead above-ground biomass accumulation at finer resolutions. This work demonstrates the potential to incorporate tools for monitoring ecohydrological processes for small catchments affected by fire across diverse ecoregions around the globe.

4.3 Science Delivery Activities

This work was disseminated through peer-reviewed publications, research conference presentations, and data repositories. The primary goal of this project was published as a thesis and journal article (1 and 2), and the secondary goal was submitted for peer- review (3):

1. Wilder, B.A., J. Lancaster, P. Cafferata, D. Coe, B. Swanson, D. Lindsay, W. Short, A.M. Kinoshita, 2020. An analytical solution for rapidly predicting post-fire peak streamflow for small watersheds in southern California. *Hydrological Processes*, 1–14. <https://doi.org/10.1002/hyp.13976>.
2. Wilder, B. A. (2021). Runoff Prediction and Ecohydrological Recovery for Small Watersheds after Fire Southern California [Unpublished master's thesis]. *San Diego State University*
3. Wilder, B.A., and A.M. Kinoshita, Monitoring Fire Severity and Ecohydrological Recovery for the 2018 Holy Fire in Southern California. *In review*.

This work resulted in the following 7 conference presentations (*indicates presenting author):

1. Wilder, B. * and A.M. Kinoshita, 2020. Post-fire Vegetation and Hydrologic Recovery in a Mediterranean Climate. American Geophysical Union Fall National Meeting, December 2020, Virtual. (Poster).
2. Wilder, B.* and A.M. Kinoshita, 2020. Flood after fire in Southern California – Incorporating Machine Learning to Identify Important Parameters for Process-based Hydrologic Models. SDSU Student Research Symposium (SRS), San Diego, CA, February (Poster, **Student received the Provost's Award in the College of Engineering**).
3. Wilder, B.* and A.M. Kinoshita, 2020. Flood after fire in Southern California – Incorporating Machine Learning to Identify Important Parameters for Process-based Hydrologic Models. 2020 IECA Annual Conference and Expo, February, Raleigh, North Carolina, USA (Poster; **Selected and sponsored to attend as a Student Moderator, Student received 1st place award**)
4. Wilder, B.* and A.M. Kinoshita, 2019. Post-wildfire peak streamflow predictions for small watersheds in southern California, USA. American Geophysical Union Fall National Meeting, December 2019, San Francisco, CA, USA. (Oral).

5. Wilder, B.* and A.M. Kinoshita, 2020. Predicting Post-Wildfire Peak Streamflow for Small Watersheds in Southern California. SDSU and USGS Collaboration workshop at Coastal and Marine Institute, San Diego, California, September 13, 2019 (Poster).
6. Wilder, B.* and A.M. Kinoshita, 2019. Predicting Post-Wildfire Peak Streamflow for Small Watersheds in Southern California. Floodplain Management Association (FMA) Conference, San Diego, California, August 2019 (Poster, Selected for the FMA Conference 2019 Student Scholarship).
7. Wilder, B.* and A.M. Kinoshita, 2019. Post-fire Peak Flow Estimates in Southern California. SDSU Student Research Symposium (SRS), San Diego, CA, March (Poster).

Science data developed for both research objectives were archived in the following repositories:

1. Wilder, B. A., A. M. Kinoshita (2021). Monitoring Fire Severity and Ecohydrological Recovery for the 2018 Holy Fire in Southern California, HydroShare, <https://doi.org/10.4211/hs.58ca489bc50f4158838394cb6f76e0e5>
2. Wilder, B. A., A. M. Kinoshita, J. T. Lancaster, P. H. Cafferata, D. B. Coe, B. J. Swanson, W. R. Short (2020). An analytical solution for rapidly predicting post-fire peak streamflows for small watersheds in southern California, HydroShare, <https://doi.org/10.4211/hs.9e38375a19cf4355aac466ccd78e8282>

5. Key Findings and Implications for Policy and Future Research

This work presented methods to improve rapid assessment and long-term prediction tools for ecohydrological processes such as streamflow and evapotranspiration (ET) in small watersheds in southern California affected by fire. We focused mainly on small watersheds (<50 km²) that were contained within the Santa Ynez Mountains, San Gabriel Mountains, San Bernardino Mountains, Santa Ana Mountains, San Jacinto Mountains, and San Diego region. A machine learning (random forest) algorithm was built with 45 watershed parameters to predict post-fire peak streamflow and compared to RCS 1949 and observed streamflow (Wilder et al., 2021). It was demonstrated that RCS 1949, a flood frequency model, overgeneralized watershed processes and did not adequately represent the spatial and temporal variability in systems affected by wildfire and extreme weather events. RCS 1949 often underpredicted peak streamflow without sediment bulking factors. A random forest flood forecasting model was developed and performed well. The improvement was expected, given the type of input data and difference in models, however, the modeling exercise demonstrated the importance and reliance on data availability of storm dependent parameters such as rainfall intensity and time after fire. The important parameters identified by the machine learning techniques were used to create a simple regression to calculate post-fire peak streamflow in small watersheds (less than 20 km²) in southern California during the first year after fire ($R^2 = 0.82$; RMSE = 6.59 cms/km²), which can be used as an interim tool by post-fire risk assessment teams.

The first objective of this study used machine learning to develop flood forecasting models to improve prediction methods for floods immediately following fires in southern California. However, prediction accuracy can be improved with more sample collection to train the machine learning model. Future efforts using machine learning would be improved greatly if there are significant increases in high resolution rainfall intensity data, sub-hourly streamgaging, and sediment loading in channels. Additionally, designing a model using a classification-based

machine learning algorithm to predict the outcomes such as debris flow, mud flow, or flooding should be explored.

Finally, to assess fire prone areas and post-fire recovery, we demonstrated the application of ECOSTRESS to characterize the 2018 Holy Fire in southern California. Using a pixel-by-pixel analysis it was demonstrated post-fire ET_{SSEBop} had lower correlation to ET_{PT-JPL} ($R^2 = 0.00$ to 0.04 ; slope = -0.10 to 0.12 ; sample size = 103) than pre-fire ($R^2 = 0.47$; slope = 0.36 ; sample size = 103). This highlights the higher spatial and temporal variability in post-fire ET caused by the large spatial heterogeneity of the burn conditions. Further, daily ET_{PT-JPL} was reduced for the burned watershed compared to the control, agreeing with previous studies for semi-arid regions that highlight a marked decrease in post-fire ET. In the second year of recovery, areas with the high soil burn severity and areas consisting of montane hardwood species had the largest summation of annual post-fire ET_{PT-JPL} .

This work demonstrated that above-ground biomass and vegetation production played a role in recovery of hydrologic processes following fires in southern California. We also showed the potential advantages of using higher spatial and temporal resolution products such as ECOSTRESS to improve vegetation assessments. Yet, more work is needed to identify areas of high-water stress and fuel build up before fire, as well as validating post-fire ET across diverse ecoregions. There is also the potential to incorporate ET_{PT-JPL} measurements as a predictor in future machine learning models to improve monitoring of annual and seasonal flows during the recovery period. Future work may also look to incorporate ground-based stations, Unmanned Aerial Systems (UAS), or satellite-based products such as ET_{PT-JPL} and others (NDVI, EVI, etc.) to improve prediction accuracy and scalability for worldwide applications.

6. Literature Cited

- Atchley, A. L., Kinoshita, A. M., Lopez, S. R., Trader, L., & Middleton, R. (2018). Simulating surface and subsurface water balance changes due to burn severity. *Vadose Zone Journal*, 17(1), 1-13. <https://doi.org/10.2136/vzj2018.05.0099>
- Baker, D. B., Richards, R. P., Loftus, T. T., & Kramer, J. W. (2004). A new flashiness index: Characteristics and applications to Midwestern rivers and streams. *Journal of the American Water Resources Association*, 40(2), 503-522. <https://doi.org/10.1111/j.1752-1688.2004.tb01046.x>
- Bell, C. E., Ditomaso, J. M., & Brooks, M. L. (2009). *Invasive plants and wildfires in Southern California*. University of California, Division of Agriculture and Natural Resources. <https://doi.org/10.3733/ucanr.8397>
- Biddinger, T., Gallegos, A., Janeki, A., TenPas, J., & Weaver, R. (2003). *BAER watershed assessment report, 2003 Grand Prix and Old Fire*. San Bernardino National Forest, unpublished report.
- Bonaccorso, B., Bordi, I., Cancelliere, A., Rossi, G., & Sutera, A. (2003). Spatial variability of drought: An analysis of the SPI in Sicily. *Water Resources Management*, 17(4), 273-296. <https://doi.org/10.1023/A:1024716530289>
- Box, G. E. P., & Cox, D. R. (1964). An analysis of transformations. *Journal of the Royal Statistical Society: Series B (Methodological)*, 26(2), 211-243. <https://doi.org/10.1111/j.2517-6161.1964.tb00553.x>
- Breiman L. (2001). Random forests. *Machine Learning*, 45(1), 5–32.
- CALFIRE. (2020). *Top 20 largest California wildfires*. https://www.fire.ca.gov/media/4jandlhh/top20_acres.pdf
- CALFIRE. (2021). *Top 20 most destructive California wildfires*. https://www.fire.ca.gov/media/t1rdhizr/top20_destruction.pdf
- CALFIRE-FRAP. (2015). *Vegetation (fveg) - CALFIRE FRAP [ds1327]*. <https://map.dfg.ca.gov/metadata/ds1327.html>
- Cannon, S. H., & DeGraff, J. (2009). The increasing wildfire and post-fire debris-flow threat in western USA, and implications for consequences of climate change. In *Landslides—disaster risk reduction* (pp. 177-190). Springer.
- Cannon, S. H., Gartner, J. E., Rupert, M. G., & Michael, J. A. (2004). *Emergency assessment of debris-flow hazards from basins burned by the Padua fire of 2003, Southern California* (US Geological Survey Open-File Report 1072). US Geological Survey.
- Cannon, S. H., Gartner, J. E., Wilson, R. C., Bowers, J. C., & Laber, J. L. (2008). Storm rainfall conditions for floods and debris flows from recently burned areas in southwestern Colorado and southern California. *Geomorphology*, 96(3-4), 250-269. <https://doi.org/10.1016/j.geomorph.2007.03.019>
- CGS [California Geological Survey]. (2002). *California geomorphic provinces* (Note 36). California Department of Conservation, California Geological Survey.
- CGS [California Geological Survey]. (2018). *Geology of California*. Author.
- Chawner, W. D. (1935). Alluvial fan flooding: The Montrose, California, Flood of 1934. *Geographical Review*, 25(2), 255-263. <https://doi.org/10.2307/209600>
- Chen, M., Senay, G. B., Singh, R. K., & Verdin, J. P. (2016). Uncertainty analysis of the Operational Simplified Surface Energy Balance (SSEBop) model at multiple flux tower sites. *Journal of Hydrology*, 536, 384-399. <https://doi.org/10.1016/j.jhydrol.2016.02.026>

- Clarke, R. T. (2002). Estimating trends in data from the Weibull and a generalized extreme value distribution. *Water Resources Research*, 38(6).
<https://doi.org/10.1029/2001wr000575>
- Cleland, D. T., Freeouf, J. A., Keys, J. E., Nowacki, G. J., Carpenter, C. A., & McNab, W. H. (2007). *Ecological subregions: Sections and subsections for the conterminous United States* (General Technical Report WO-76D). U.S. Department of Agriculture, Forest Service.
- Coalitions & Collaboratives, Inc. (Producer). (2020). *After the flames* [Video].
<https://aftertheflames.com/science-sessionresources/>
- Debano, L. F. (2000). The role of fire and soil heating on water repellency in wildland environments: A review. *Journal of Hydrology*, 231-232, 195-206.
[https://doi.org/10.1016/S0022-1694\(00\)00194-3](https://doi.org/10.1016/S0022-1694(00)00194-3)
- Dettinger, M. (2011). Climate change, atmospheric rivers, and floods in California - a multimodel analysis of storm frequency and magnitude changes. *Journal of the American Water Resources Association*, 47(3), 514-523.
<https://doi.org/10.1111/j.1752-1688.2011.00546.x>
- DiBiase, R. A., & Lamb, M. P. (2020). Dry sediment loading of headwater channels fuels post-wildfire debris flows in bedrock landscapes. *Geology*, 48(2), 189-193.
<https://doi.org/10.1130/G46847.1>
- Doerr, S. H., Shakesby, R. A., & Macdonald, L. H. (2009). Soil water repellency: A key factor in post-fire erosion. In A. Cerda & P. R. Robichaud (Eds.), *Fire effects on soils and restoration strategies*. Routledge.
- Doerr, S. H., Shakesby, R. A., & Walsh, R. P. D. (2000). Soil water repellency: Its causes, characteristics and hydro-geomorphological significance. *Earth Science Reviews*, 51(1-4), 33-65. [https://doi.org/10.1016/S0012-8252\(00\)00011-8](https://doi.org/10.1016/S0012-8252(00)00011-8)
- Dong, C., MacDonald, G. M., Willis, K., Gillespie, T. W., Okin, G. S., & Williams, A. P. (2019). Vegetation responses to 2012–2016 drought in Northern and Southern California. *Geophysical Research Letters*, 46(7), 3810-3821.
<https://doi.org/10.1029/2019GL082137>
- Feller, W. (1968). *An introduction to probability theory and its applications* (Vol. 1). John Wiley & Sons.
- Fernández, C., & Vega, J. A. (2016). Modelling the effect of soil burn severity on soil erosion at hillslope scale in the first year following wildfire in NW Spain. *Earth Surface Processes and Landforms*, 41(7), 928-935. <https://doi.org/10.1002/esp.3876>
- Fernández-Guisuraga, J. M., Sanz-Ablanedo, E., Suárez-Seoane, S., & Calvo, L. (2018). Using unmanned aerial vehicles in postfire vegetation survey campaigns through large and heterogeneous areas: Opportunities and challenges. *Sensors*, 18(2), 586.
<https://doi.org/10.3390/s18020586>
- Fisher, J. B., Lee, B., Purdy, A. J., Halverson, G. H., Dohlen, M. B., Cawse-Nicholson, K., Wang, A., Anderson, R. G., Aragon, B., Arain, M. A., Baldocchi, D. D., Baker, J. M., Barral, H., Bernacchi, C. J., Bernhofer, C., Biraud, S. C., Bohrer, G., Brunsell, N., Cappelaere, B., ... Hook, S. (2020). Ecostress: NASA's next generation mission to measure evapotranspiration from the International Space Station. *Water Resources Research*, 56(4), e2019WR026058. <https://doi.org/10.1029/2019WR026058>
- Flynn, K., Kirby, W., & Hummel, P. (2006). *User's manual for program PeakFQ, annual flood-frequency analysis using bulletin 17B guidelines* (Chapter 4 of Book 4, Section

- B). U.S. Department of the Interior, U.S. Geological Survey
- Foltz, R. B., Robichaud, P. R., & Rhee, H. (2009). *A synthesis of post-fire road treatments for BAER teams: methods, treatment effectiveness, and decision making tools for rehabilitation* (General Technical Report RMRS-228). U.S. Department of Agriculture, Forest Service, Rocky Mountain Research Station.
- FRAP [Fire and Resource Assessment Program]. (2015). *State fire perimeter database*. California Department of Forestry and Fire Protection.
- FRAP [Fire and Resource Assessment Program]. (2018). *California's forests and rangelands: 2017 assessment*. California Department of Forestry and Fire Protection.
- Gabet, E. J. (2003). Post-fire thin debris flows: Sediment transport and numerical modelling. *Earth Surface Processes and Landforms: The Journal of the British Geomorphological Research Group*, 28(12), 1341-1348.
- Gartner, J. E., Cannon, S. H., & Santi, P. M. (2014). Empirical models for predicting volumes of sediment deposited by debris flows and sediment-laden floods in the transverse ranges of southern California. *Engineering Geology*, 176(24), 45-56. <https://doi.org/10.1016/j.enggeo.2014.04.008>
- Goodrich, D. C., Burns, I. S., Unkrich, C. L., Semmens, D. J., Guertin, D. P., Hernandez, M., & Levick, L. R. (2012). KINEROS2/AGWA: model use, calibration, and validation. *Transactions of the ASABE*, 55(4), 1561-1574.
- Goodrich, D., Canfield, H. E., Burns, I. S., Semmens, D., Miller, S., Hernandez, M., Levick, L. R., Guertin, W. G., & Kepner, W. (2005, July). Rapid post-fire hydrologic watershed assessment using the AGWA GIS-based hydrologic modeling tool. In G. E. Moglen (Ed.), *Managing watersheds for human and natural impacts: engineering, ecological, and economic challenges* (pp. 1-12). ASCE.
- Gorelick, N., Hancher, M., Dixon, M., Ilyushchenko, S., Thau, D., & Moore, R. (2017). Google earth engine: Planetary-scale geospatial analysis for everyone. *Remote Sensing of Environment*, 202, 18-27. <https://doi.org/10.1016/j.rse.2017.06.031>
- Guarín, A., & Taylor, A. H. (2005). Drought triggered tree mortality in mixed conifer forests in Yosemite National Park, California, USA. *Forest Ecology and Management*, 218(1-3), 229-244. <https://doi.org/10.1016/j.foreco.2005.07.014>
- Guilinger, J. J., Gray, A. B., Barth, N. C., & Fong, B. T. (2020). The evolution of sediment sources over a sequence of postfire sediment-laden flows revealed through repeat high-resolution change detection. *Journal of Geophysical Research: Earth Surface*, 125(10), e2020JF005527. <https://doi.org/10.1029/2020JF005527>
- Harden, J. W., & Matti, J. C. (1989). Holocene and late Pleistocene slip rates on the San Andreas fault in Yucaipa, California, using displaced alluvial-fan deposits and soil chronology. *Geological Society of America Bulletin*. [https://doi.org/10.1130/0016-7606\(1989\)101<1107:HALPSR>2.3.CO;2](https://doi.org/10.1130/0016-7606(1989)101<1107:HALPSR>2.3.CO;2)
- Hogue, T. S., Sorooshian, S., Gupta, H., Holz, A., & Braatz, D. (2000). A multistep automatic calibration scheme for river forecasting models. *Journal of Hydrometeorology*, 1(6). [https://doi.org/10.1175/1525-7541\(2000\)001<0524:AMACSF>2.0.CO;2](https://doi.org/10.1175/1525-7541(2000)001<0524:AMACSF>2.0.CO;2)
- Horton, R. E. (1945). Erosional development of streams and their drainage basins; hydrophysical approach to quantitative morphology. *Geological Society of America Bulletin*, 56(3), 275-370.
- Huffman, E. L., MacDonald, L. H., & Stednick, J. D. (2001). Strength and persistence of fire-

- induced soil hydrophobicity under ponderosa and lodgepole pine, Colorado Front Range. *Hydrological Processes*, 15, 2877-2892. <https://doi.org/10.1002/hyp.379>
- Johansen, M. P., Hakonson, T. E., & Breshears, D. D. (2001). Post-fire runoff and erosion from rainfall simulation: Contrasting forests with shrublands and grasslands. *Hydrological Processes*, 15(15), 2953-2965.
- Kean, J. W., Staley, D. M., Lancaster, J. T., Rengers, F. K., Swanson, B. J., Coe, J. A., Hernandez, J. L., Sigman, A. J., Allstadt, K. E., & Lindsay, D. N. (2019). *Inundation, flow dynamics, and damage in the 9 January 2018 Montecito debris-flow event, California, USA: Opportunities and challenges for post-wildfire risk assessment*. Geosphere. <https://doi.org/10.1130/GES02048.1>
- Keeley, J. E. (2009). Fire intensity, fire severity and burn severity: A brief review and suggested usage. *International Journal of Wildland Fire*, 18(1), 116-126. <https://doi.org/10.1071/WF07049>
- Keeley, J. E., & Keeley, S. C. (1981). Post-fire regeneration of southern California Chaparral. *American Journal of Botany*, 68(4), 524-530. <https://doi.org/10.2307/2443028>
- Keeley, J. E., Fotheringham, C. J., & Moritz, M. A. (2004). Lessons from the October 2003 wildfires in Southern California. *Journal of Forestry*, 102(7), 26-31. <https://doi.org/10.1093/jof/102.7.26>
- Keller, E. A., Valentine, D. W., & Gibbs, D. R. (1997). Hydrological response of small watersheds following the Southern California painted cave fire of June 1990. *Hydrological Processes*, 11(4), 401-414.
- Kinoshita, A. M., & Hogue, T. S. (2011). Spatial and temporal controls on post-fire hydrologic recovery in Southern California watersheds. *Catena*, 87(2), 240-252.. <https://doi.org/10.1016/j.catena.2011.06.005>
- Kinoshita, A. M., & Hogue, T. S. (2015). Increased dry season water yield in burned watersheds in Southern California. *Environmental Research Letters*, 10(1). <https://doi.org/10.1088/1748-9326/10/1/014003>
- Kinoshita, A. M., Chin, A., Simon, G. L., Briles, C., Hogue, T. S., O'Dowd, A. P., Gerlak, A. K., & Albornoz, A. U. (2016). Wildfire, water, and society: Toward integrative research in the "Anthropocene." *Anthropocene*, 16(2016), 166-27. <https://doi.org/10.1016/j.ancene.2016.09.001>
- Kinoshita, A. M., Hogue, T. S., & Napper, C. (2014). Evaluating pre- and post-fire peak discharge predictions across western U.S. watersheds. *Journal of the American Water Resources Association*, 50(6), 1540-1557. <https://doi.org/10.1111/jawr.12226>
- Kohli, G., Lee, C. M., Fisher, J. B., Halverson, G., Variano, E., Jin, Y., Carney, D., Wilder, B. A., & Kinoshita, A. M. (2020). ECOSTRESS and CIMIS: A Comparison of Potential and Reference Evapotranspiration in Riverside County, California. *Remote Sensing*, 12(24), 4126. <https://doi.org/10.3390/rs12244126>
- Lamjiri, M. A., Dettinger, M. D., Ralph, F. M., Oakley, N. S., & Rutz, J. J. (2018). Hourly analyses of the large storms and atmospheric rivers that provide most of California's precipitation in only 10 to 100 hours per year. *San Francisco Estuary and Watershed Science*, 16(4), 1-17. <https://doi.org/10.15447/sfews.2018v16iss4art1>
- Lancaster, J. T., Swanson, B. J., Lukashova, S., Oakley, N., Lee, J. B., Spangler, E., Hernandez, J. L., Olson, B. P. E., DeFrisco, M. J., Lindsay, D. J., Schwartz, Y. J., McCrea, S. E., Roffers, P. D., & C. M. Tran. (in press). *Observations and analyses of the 9 January 2018 debris flow disaster, Santa Barbara County*. Environmental and

- Engineering Geoscience.
- Lavé, J., & Burbank, D. (2004). Denudation processes and rates in the Transverse Ranges, southern California: Erosional response of a transitional landscape to external and anthropogenic forcing. *Journal of Geophysical Research: Earth Surface*, 109(F1). <https://doi.org/10.1029/2003jf000023>
- Lentile, L. B., Morgan, P., Hudak, A. T., Bobbitt, M. J., Lewis, S. A., Smith, A. M., & Robichaud, P. R. (2007). Post-fire burn severity and vegetation response following eight large wildfires across the western United States. *Fire Ecology*, 3(1), 91-108. <https://doi.org/10.4996/fireecology.0301091>
- Lewis, S. A., Wu, J. Q., & Robichaud, P. R. (2006). Assessing burn severity and comparing soil water repellency, Hayman Fire, Colorado. *Hydrological Processes*, 20(1), 1-16. <https://doi.org/10.1002/hyp.5880>
- Ma, Q., Bales, R. C., Rungee, J., Conklin, M. H., Collins, B. M., & Goulden, M. L. (2020). Wildfire controls on evapotranspiration in California's Sierra Nevada. *Journal of Hydrology*, 590, 125364. <https://doi.org/10.1016/j.jhydrol.2020.125364>
- MacDonald, L. H., & Huffman, E. L. (2004). Post-fire soil water repellency. *Soil Science Society of America Journal*, 68(5), 1729-1734.
- Mayor, A. G., Bautista, S., Llovet, J., & Bellot, J. (2007). Post-fire hydrological and erosional responses of a Mediterranean landscape: Seven years of watershed-scale dynamics. *Catena*, 71(1), 68-75. <https://doi.org/10.1016/j.catena.2006.10.006>
- McKay, L., Bondelid, T., Dewald, T., Rea, A., Johnston, C., & Moore, R. (2015). *NHDPlus version 2: User guide* (data model version 2.1). Horizon Systems.
- McMillan, H. (2020). Linking hydrologic signatures to hydrologic processes: A review. *Hydrological Processes*, 34(6), 1393-1409. <https://doi.org/10.1002/hyp.13632>
- Miller, J. D., Knapp, E. E., Key, C. H., Skinner, C. N., Isbell, C. J., Creasy, R. M., & Sherlock, J. W. (2009). Calibration and validation of the relative differenced Normalized Burn Ratio (RdNBR) to three measures of fire severity in the Sierra Nevada and Klamath Mountains, California, USA. *Remote Sensing of Environment*, 113(3), 645-656.
- Miller, J. D., Nyhan, J. W., & Yool, S. R. (2003). Modeling potential erosion due to the Cerro Grande Fire with a GIS-based implementation of the Revised Universal Soil Loss Equation. *International Journal of Wildland Fire*, 12(1), 85-100.
- Miller, N. L., & Schlegel, N. J. (2006). Climate change projected fire weather sensitivity: California Santa Ana wind occurrence. *Geophysical Research Letters*, 33(15). <https://doi.org/10.1029/2006GL025808>
- Miller, V. C. (1953). *Quantitative geomorphic study of drainage basin characteristics in the Clinch Mountain area, Virginia and Tennessee* [Technical report]. Columbia University, Department of Geology.
- Milly, P. C. D., Betancourt, J., Falkenmark, M., Hirsch, R. M., Kundzewicz, Z. W., Lettenmaier, D. P., & Stouffer, R. J. (2008). Climate change: Stationarity is dead: Whither water management? *Science*, 319(5863), 573-574. <https://doi.org/10.1126/science.1151915>
- Moody, J. A. (2012). *An analytical method for predicting postwildfire peak discharges*. USGS Investigations Report.
- Moody, J. A., & Martin, D. A. (2001). Initial hydrologic and geomorphic response following a wildfire in the Colorado front range. *Earth Surface Processes and Landforms*,

- 26(10), 1049-1070. <https://doi.org/10.1002/esp.253>
- Moody, J. A., Martin, D. A., Haire, S. L., & Kinner, D. A. (2008). Linking runoff response to burn severity after a wildfire. *Hydrological Processes: An International Journal*, 22(13), 2063-2074.
- Moody, J. A., Shakesby, R. A., Robichaud, P. R., Cannon, S. H., & Martin, D. A. (2013). Current research issues related to post-wildfire runoff and erosion processes. *Earth-Science Reviews*, 122(July 2013), 10-37. <https://doi.org/10.1016/j.earscirev.2013.03.004>
- Moody, J. A., Shakesby, R. A., Robichaud, P. R., Cannon, S. H., & Martin, D. A. (2013). Current research issues related to post-wildfire runoff and erosion processes. *EarthScience Reviews*, 122, 10-37.
- Moore, M., Bigginger, T., Thornton, J., Wright, K., & Stewart, C. (2009). *BAER watershed assessment report, Station Fire* [Unpublished report].
- Musselman, K. N., Molotch, N. P., & Margulis, S. A. (2017). Snowmelt response to simulated warming across a large elevation gradient, southern Sierra Nevada, California. *The Cryosphere*, 11(6), 2847–2866.
- Neary, D. G., Ryan, K. C., & DeBano, L. F. (2005). *Wildland fire in ecosystems: Effects of fire on soils and water* (General Technical Reports. RMRS-GTR42-vol. 4.). US Department of Agriculture, Forest Service, Rocky Mountain Research Station.
- Neiman, P. J., Ralph, F. M., Wick, G. A., Kuo, Y. H., Wee, T. K., Ma, Z., Taylor, G. H., & Dettinger, M. D. (2008). Diagnosis of an intense atmospheric river impacting the pacific northwest: Storm summary and offshore vertical structure observed with COSMIC satellite retrievals. *Monthly Weather Review*, 136(11). <https://doi.org/10.1175/2008MWR2550.1>
- O'Connor, J. E., & Costa, J. E. (2004). *The world's largest floods, past and present: Their causes and magnitudes*. US Geological Survey Circular. <https://doi.org/10.3133/cir1254>
- Oakley, N. S., Lancaster, J. T., Kaplan, M. L., & Ralph, F. M. (2017). Synoptic conditions associated with cool season post-fire debris flows in the Transverse Ranges of southern California. *Natural Hazards*, 88, 327-354. <https://doi.org/10.1007/s11069-017-2867-6>
- Obrist, D., Yakir, D., & Arnone, J. A. (2004). Temporal and spatial patterns of soil water following wildfire-induced changes in plant communities in the Great Basin in Nevada, USA. *Plant and Soil*, 262, 1-12. <https://doi.org/10.1023/B:PLSO.0000037026.93675.a2>
- Orfanidis, S. J. (1996). *Introduction to signal processing*. Prentice Hall.
- Pal, M. (2005). Random forest classifier for remote sensing classification. *International Journal of Remote Sensing*, 26(1), 217-222. <https://doi.org/10.1080/01431160412331269698>
- Parrett, C., Veilleux, A., Stedinger, J. R., Barth, N. A., Knifong, D. L., & Ferris, J. C. (2011). *Regional skew for California, and flood frequency for selected sites in the Sacramento-San Joaquin River Basin, based on data through water year 2006*. U. S. Geological Survey.
- Parsons, A., Robichaud, P. R., Lewis, S. A., Napper, C., & Clark, J. T. (2010). *Field guide for mapping post-fire soil burn severity* (Gen. Tech. Rep. RMRS-GTR-243). U.S. Department of Agriculture, Forest Service, Rocky Mountain Research Station.
- Peel, M. C., Finlayson, B. L., & McMahon, T. A. (2007). Updated world map of the Köppen-

- Geiger climate classification. *Hydrology and Earth System Sciences*, 11(5), 1633-1644. <https://doi.org/10.5194/hess-11-1633-2007>
- Pierson, T. (2005). *Distinguishing between debris flows and floods from field evidence in small watersheds*. U.S. Geological Survey.
- Poon, P. K., & Kinoshita, A. M. (2018). Spatial and temporal evapotranspiration trends after wildfire in semi-arid landscapes. *Journal of Hydrology*, 559, 71-83. <https://doi.org/10.1016/j.jhydrol.2018.02.023>
- Prater, M. R., & DeLucia, E. H. (2006). Non-native grasses alter evapotranspiration and energy balance in Great Basin sagebrush communities. *Agricultural and Forest Meteorology*, 139(1-2), 154-163. <https://doi.org/10.1016/j.agrformet.2006.08.014>
- Prein, A. F., Rasmussen, R. M., Ikeda, K., Liu, C., Clark, M. P., & Holland, G. J. (2017). The future intensification of hourly precipitation extremes. *Nature Climate Change*, 7, 48-52. <https://doi.org/10.1038/nclimate3168>
- Radeloff, V. C., Hammer, R. B., Stewart, S. I., Fried, J. S., Holcomb, S. S., & McKeefry, J. F. (2005). The wildland-urban interface in the United States. *Ecological Applications*, 15(3), 799-805. <https://doi.org/10.1890/04-1413>
- Ralph, F. M., & Dettinger, M. D. (2012). Historical and national perspectives on extreme west coast precipitation associated with atmospheric rivers during December 2010. *Bulletin of the American Meteorological Society*, 93(6), 783-790. <https://doi.org/10.1175/BAMS-D-11-00188.1>
- Raphael, M. N. (2003). The Santa Ana Winds of California. *Earth Interactions*, 7(8), 1-13. [https://doi.org/10.1175/1087-3562\(2003\)007<0001:tsawoc>2.0.co;2](https://doi.org/10.1175/1087-3562(2003)007<0001:tsawoc>2.0.co;2)
- Reback, J., McKinney, W., jbrockmendel, Van den Bossche, J., Augspurger, T., Cloud, P., gyoung, Sinhrks, Klein, A., Roeschke, M., Hawkins, S., Tratner, J., She, C., Ayd, W., Petersen, T., Garcia, M., Schendel, J., Hayden, A., MomIsBestFriend, ...
 Mehyar, M. (2020, March 18). *pandas-dev/pandas: Pandas 1.0.3 (Version v1.0.3)* [Software]. Zenodo. <http://doi.org/10.5281/zenodo.3715232>
- Robichaud, P. R., Elliot, W. J., Pierson, F. B., Hall, D. E., & Moffet, C. A. (2007). Predicting postfire erosion and mitigation effectiveness with a web-based probabilistic erosion model. *Catena*, 71(2), 229-241. <https://doi.org/10.1016/j.catena.2007.03.003>
- Robichaud, Peter R., Elliot, W. J., & Wagenbrenner, J. W. (2011, September 18-21). *Probabilistic soil erosion modeling using the Erosion Risk Management Tool (ERMiT) after wildfires* [Paper presentation]. International Symposium on Erosion and Landscape Evolution, Anchorage, Alaska.
- Rowe, P. B., Countryman, O. M., & Storey, H. C. (1949). *Probable peak discharges and erosion rates from southern California watersheds as influenced by fire*. US Department of Agriculture, Forest Service.
- Safford, H. D., & Van de Water, K. M. (2013). *Using Fire Return Interval Departure (FRID) analysis to map spatial and temporal changes in fire frequency on National Forest lands in California* (Res. Pap. PSW-RP-266). Department of Agriculture, Forest Service, Pacific Southwest Research Station.
- Savoca, M. E., Senay, G. B., Maupin, M. A., Kenny, J. F., & Perry, C. A. (2013). *Actual evapotranspiration modeling using the operational simplified surface energy balance (SSEBop) approach* (U.S Geological Survey Scientific Investigations Report 2013-5126). U.S. Geological Survey.
- Saxe, S., Hogue, T. S., & Hay, L. (2018). Characterization and evaluation of controls on post-

- fire streamflow response across western US watersheds. *Hydrology and Earth System Sciences*, 22(2), 1221-1237. <https://doi.org/10.5194/hess-22-1221-2018>
- Schmidt, L., Heße, F., Attinger, S., & Kumar, R. (2020). Challenges in applying machine learning models for hydrological inference: A case study for flooding events across Germany. *Water Resources Research*, 56(5). <https://doi.org/10.1029/2019WR025924>
- Schumm, S. A. (1956). Evolution of drainage systems and slopes in badlands at Perth Amboy, New Jersey. *Geological society of America Bulletin*, 67(5), 597-646.
- Scott, K. M., & Williams, R. P. (1978). *Erosion and sediment yields in the Transverse Ranges, southern California*. US Government Printing Office.
- Shakesby, R. A., Moody, J. A., Martin, D. A., & Robichaud, P. R. (2016). Synthesising empirical results to improve predictions of post-wildfire runoff and erosion response. *International Journal of Wildland Fire*, 26(3), 257-261. <https://doi.org/10.1071/WF16021>
- Shuirman, G., & Slosson, J. E. (1992). *Forensic engineering – Environmental case histories for engineers and geologists*. Academic Press.
- Soulis, K. X., Generali, K. A., Papadaki, C., Theodoropoulos, C., & Psomiadis, E. (2021). Hydrological response of natural mediterranean watersheds to forest fires. *Hydrology*, 8(1), 15. <https://doi.org/10.3390/hydrology8010015>
- Staley, D. M., Kean, J. W., Cannon, S. H., Schmidt, K. M., & Laber, J. L. (2013). Objective definition of rainfall intensity-duration thresholds for the initiation of post-fire debris flows in southern California. *Landslides*, 10, 547-562. <https://doi.org/10.1007/s10346-012-0341-9>
- Staley, D. M., Negri, J. A., Kean, J. W., Laber, J. L., Tillery, A. C., & Youberg, A. M. (2017). Prediction of spatially explicit rainfall intensity–duration thresholds for postfire debris-flow generation in the western United States. *Geomorphology*, 278, 149-162. <https://doi.org/10.1016/j.geomorph.2016.10.019>
- Stavros, E. N., Bloom, A. A., Brown, T., Coen, J., Dennison, P., Giglio, L., Green, R., Hinkley, E., Holden, Z., Hook, S., Johnson, W., Miller, M. E., Petersen, B., Quayle, B., Ramirez, C., Randerson, J., Schimel, D., Schroeder, W., Soja, A., & Tosca, M. (2017). *The role of fire in the Earth System*. NASA.
- Steel, Z. L., Safford, H. D., & Viers, J. H. (2015). The fire frequency-severity relationship and the legacy of fire suppression in California forests. *Ecosphere*, 6(1), 1-23. <https://doi.org/10.1890/ES14-00224.1>
- Syphard, A. D., Radeloff, V. C., Keeley, J. E., Hawbaker, T. J., Clayton, M. K., Stewart, S. I., & Hammer, R. B. (2007). Human influence on California fire regimes. *Ecological Applications*, 17(5), 1388-1402. <https://doi.org/10.1890/06-1128.1>
- Tarboton, D. G. (2003). Terrain analysis using digital elevation models in hydrology [Conference paper]. *23rd ESRI International Users Conference, San Diego, California*.
- Taylor, A. H., Trouet, V., & Skinner, C. N. (2008). Climatic influences on fire regimes in montane forests of the southern Cascades, California, USA. *International Journal of Wildland Fire*, 17(1), 60-71. <https://doi.org/10.1071/WF07033>
- Travis, B., Teal, M., & Gusman, J. (2012, May 20-24). *Best methods and inherent limitations of bulked flow modeling with HEC-RAS* [Paper presentation]. World Environmental and Water Resources Congress 2012, Albuquerque, New Mexico.
- USDA Forest Service. (2013). *Burned area emergency response tools*.

- <https://forest.moscowfsl.wsu.edu/BAERTOOLS/ROADTRT/Peakflow/CN/supplement.html>
- USFS. (2020). *Round table discussion*. Holy Fire Research Symposium at United States Forest Service Pacific Southwest Research Station, Riverside, California
- Uyeda, K. A., Stow, D. A., & Riggan, P. J. (2015). Tracking MODIS NDVI time series to estimate fuel accumulation. *Remote Sensing Letters*, 6(8), 587-596.
<https://doi.org/10.1080/2150704X.2015.1063736>
- Van de Water, K. M., & Safford, H. D. (2011). A summary of fire frequency estimates for California vegetation before Euro-American settlement. *Fire Ecology*, 7, 266-58.
<https://doi.org/10.4996/fireecology.0703026>
- Vieira, D. C. S., Fernández, C., Vega, J. A., & Keizer, J. J. (2015). Does soil burn severity affect the post-fire runoff and interrill erosion response? A review based on metaanalysis of field rainfall simulation data. *Journal of Hydrology*, 523, 452-464.
<https://doi.org/10.1016/j.jhydrol.2015.01.071>
- Vo, V. D., & Kinoshita, A. M. (2020). Remote sensing of vegetation conditions after postfire mulch treatments. *Journal of Environmental Management*, 260, 109993.
<https://doi.org/10.1016/j.jenvman.2019.109993>
- Wagenbrenner, J. W. (2013). *Post-fire stream channel processes: Changes in runoff rates, sediment delivery across spatial scales, and mitigation effectiveness* [Doctoral dissertation, Washington State University]. Washington State University Libraries.
<http://hdl.handle.net/2376/4931>
- Wells, W. G. (1981, January 25-31). Some effects of brushfires on erosion processes in coastal southern California: Erosion and sediment transport in Pacific Rim steplands [Paper presentation]. Proceedings of the Christchurch Symposium, Christchurch, New Zealand.
- Wells, W. G. (1987). The effects of fire on the generation of debris flows in southern California. *GSA Reviews in Engineering Geology*, 7, 105-114.
<https://doi.org/10.1130/REG7-p105>
- Wenger, S. J., & Fowler, L. (2000). *Protecting stream and river corridors: creating effective local riparian buffer ordinances*. Carl Vinson Institute of Government, The University of Georgia.
- WERT (Watershed Emergency Response Team). (2018a). *Holy Fire— Watershed Emergency Response Team final report, CA-RRU-100160*. ACWI.
- WERT (Watershed Emergency Response Team). (2018b). *Woolsey and Hill Fires— Watershed Emergency Response Team final report, CA-VNC091023 and CA-VNC090993*. ACWI.
- WERT (Watershed Emergency Response Team). (2019a). *Cave Fire— Watershed Emergency Response Team final report, CA-LPF-002908*. ACWI.
- WERT (Watershed Emergency Response Team). (2019b). *Saddle Ridge Fire—Watershed Emergency Response Team final report, CA-LFD00001582*. ACWI.
- Westerling, A. L., Hidalgo, H. G., Cayan, D. R., & Swetnam, T. W. (2006). Warming and earlier spring increase Western U.S. forest wildfire activity. *Science*, 313(5789), 940943. <https://doi.org/10.1126/science.1128834>
- Wilder, B. A., Lancaster, J. T., Cafferata, P. H., Coe, D. B., Swanson, B. J., Lindsay, D. N., Short, W. R. & Kinoshita, A. M. (2021). An analytical solution for rapidly predicting post-fire peak streamflow for small watersheds in southern California. *Hydrological*

- Processes*, 35(1), e13976. <https://doi.org/10.1002/hyp.13976>
- Williams, A. P., Abatzoglou, J. T., Gershunov, A., Guzman-Morales, J., Bishop, D. A., Balch, J. K., & Lettenmaier, D. P. (2019). Observed impacts of anthropogenic climate change on wildfire in California. *Earth's Future*, 7(8), 892-910. <https://doi.org/10.1029/2019EF001210>
- Wills, C. J., Perez, F. G., & Gutierrez, C. I. (2011). Susceptibility to deep-seated landslides in California. *California Geological Survey Map Sheet*.
- Wine, M. L., Cadol, D., & Makhnin, O. (2018). In ecoregions across western USA streamflow increases during post-wildfire recovery. *Environmental Research Letters*, 13(1), 014010. <https://doi.org/10.1088/1748-9326/aa9c5a>
- Wittenberg, L., Malkinson, D., Beerli, O., Halutzky, A., & Tesler, N. (2007). Spatial and temporal patterns of vegetation recovery following sequences of forest fires in a Mediterranean landscape, Mt. Carmel Israel. *Catena*, 71(1), 76-83. <https://doi.org/10.1016/j.catena.2006.10.007>
- Wohlgemuth, P. (2016). *Long-term hydrologic research on the San Dimas Experimental Forest, southern California: Lessons learned and future directions* [Conference proceedings]. The Fifth Interagency Conference on Research in the Watersheds. North Charleston, SC, United States.
- Wohlgemuth, P. (2016, March). Long-term hydrologic research on the San Dimas Experimental Forest, southern California: Lessons learned and future directions. In C. E. Stringer, K. W. Krauss, & J. S. Latimer (Eds.), *Headwaters to estuaries: Advances in watershed science and management-Proceedings of the Fifth Interagency Conference on Research in the Watersheds* (Vol. 211; pp. 227–232). US Department of Agriculture Forest Service, Southern Research Station.
- World Meteorological Organization. (2012). *Standardized precipitation index user guide* (M. Svoboda, M. Hayes and D. Wood). Author.

Appendix A: Contact Information for Key Project Personnel

PI

Name: Alicia M. Kinoshita

Institution: San Diego State University

Email: akinoshita@sdsu.edu

SI

Name: Brenton A. Wilder

Institution: San Diego State University

Email: bwilder6623@sdsu.edu

Co-authors

Names: Jeremy T. Lancaster, Peter H. Cafferata, Drew B.R. Coe, Brian J. Swanson, Donald N. Lindsay, William R Short

Appendix B: List of Science Delivery Products

Refer to Section 4.3 of this report.

Appendix C: Metadata

Metadata is included in links provided within Section 4.3 of this final report. Data delivery differs from that provided in data management plan. We utilized HydroShare, a National Science Foundation funded hydrological database for research scientists, to archive our data. HydroShare can be readily accessed by the general science community. The HydroShare repositories are linked to the corresponding paper and published under the same name. The second paper and data, “Monitoring Fire Severity and Ecohydrological Recovery for the 2018 Holy Fire in Southern California,” is in peer review.